

Non-universal gaugino masses: a signal-based analysis for the Large Hadron Collider

Subhaditya Bhattacharya¹, Aresh Krishna Datta² and Biswarup Mukhopadhyaya³

Regional Centre for Accelerator-based Particle Physics

Harish-Chandra Research Institute

Chhatnag Road, Jhusi, Allahabad - 211 019, India

Abstract

We discuss the signals at the Large Hadron Collider (LHC) for scenarios with non-universal gaugino masses in supersymmetric (SUSY) theories. We perform a multichannel analysis, and consider the ratios of event rates in different channels such as *jets* + \cancel{E}_T , *same* - and *opposite-sign dileptons* + *jets* + \cancel{E}_T , as well as *single-lepton* and *trilepton* final states together with *jets* + \cancel{E}_T . Low-energy SUSY spectra corresponding to high-scale gaugino non-universality arising from different breaking schemes of SU(5) as well as SO(10) Grand Unified (GUT) SUSY models are considered, with both degenerate low-energy sfermion masses and those arising from a supergravity scenario. We present the numerical predictions over a wide range of the parameter space using the event generator `Pythia`, specifying the event selection criteria and pointing out regions where signals are likely to be beset with backgrounds. Certain broad features emerge from the study, which may be useful in identifying the signatures of different GUT breaking schemes and distinguishing them from a situation with a universal gaugino mass at high scale. The absolute values of the predicted event rates for different scenarios are presented together with the various event ratios, so that these can also be used whenever necessary.

¹E-mail: subha@mri.ernet.in

²E-mail: asesh@mri.ernet.in

³E-mail: biswarup@mri.ernet.in

1 Introduction

In its bid to unravel new laws of physics around the TeV scale, the Large Hadron Collider (LHC) experiment will place considerable emphasis on the search for supersymmetry (SUSY) [1, 2, 3]. Apart from stabilizing the electroweak symmetry breaking sector and providing a rather tantalizing hint of Grand Unification, SUSY (in the R -parity conserving version) also provides a cold dark matter candidate in the form of the stable lightest supersymmetric particle (LSP) [4]. With this in view, the SUSY signals that are most frequently talked about are those where a large amount of missing (transverse) momentum is carried away by a pair of LSP's resulting from decay chains of superparticles produced in the initial hard scattering process [2, 4]. The missing energy is accompanied by hard jets and/or leptons, and their relative numbers as well as signs in the observed final states are expected to direct us to specific regions of the 'signature space', indicating, in turn, where one stands in the parameter space of the overseeing SUSY theory [5, 6, 7, 8, 9, 10, 11].

Locating oneself correctly in the signature space also helps one in knowing whether some of the usual or simplifying assumptions made about SUSY are actually tenable. For example, signals can be qualitatively different if R -parity (with $R = (-1)^{3B+L+2S}$) is violated [12], or the LSP is, contrary to common expectations, not the lightest neutralino (χ_1^0) [13]. Very heavy scalars can also warrant a different analysis of SUSY signals [14, 15, 16]. Similarly, signals may also be quite different if, instead of the supergravity (SUGRA) scheme controlling SUSY breaking, gauge mediated SUSY breaking (GMSB) [4, 17] or anomaly mediated SUSY breaking (AMSB) [4, 18] is operative. A more difficult problem is, however, posed if the signals are not qualitatively new but are found to differ from usual expectations only on detailed quantitative scrutiny. Here we undertake an analysis of one such situation, where, contrary to the most popular outcome of SUSY embedded in a Grand Unified Theory (GUT) framework, the gaugino masses at the high scale are *not* unified. [19, 20].

In the simplest SUGRA models, all low-scale parameters are derived from a universal gaugino mass ($M_{1/2}$), a universal scalar mass (m_0), the trilinear soft SUSY-breaking parameter (A_0) and the sign of the Higgsino mass parameter ($\text{sgn}(\mu)$) for each value of $\tan\beta$, the ratio of the two Higgs vacuum expectation values [4]. A universal gaugino mass occurs in the simplest form of a SUSY GUT. Its immediate consequence is that the three low-energy gaugino masses corresponding to SU(3), SU(2) and U(1) are in the ratio of the corresponding fine-structure constants: $\frac{M_3}{\alpha_3} = \frac{M_2}{\alpha_2} = \frac{M_1}{\alpha_1}$ [4]. This relation governs the low-energy chargino and neutralino masses vis-a-vis the gluino mass. It has profound implications on the strengths of different types of signals, since gluinos are liable to be copiously produced

at the LHC, and the cascades initiated by them involve the charginos and neutralinos at various stages [3, 7]. Therefore, if gaugino mass universality at high scale does not hold, it means that both the spectrum and the compositions of the charginos and neutralinos are subject to marked variations, so that the final states have different rates compared to the universal case both through kinematics and dynamics.

While departure from universality may well indicate that one is not facing a SUSY GUT scenario, it may, interestingly, still be the consequence of a GUT framework. The gaugino masses arise from the gauge kinetic function whose trivial nature, as we shall see in the next section, implies a universal gaugino mass when SUSY is broken at high scale. This is possible if the combination of hidden sector fields involved in the function is a singlet under the GUT group. However, it is always possible to generate mass terms via higher GUT representations, which in turn create inequality among M_1 , M_2 and M_3 at the high scale itself. It is also possible to have more than one GUT representations involved in SUSY breaking, in which case the non-universality arises from a linear combination of the effects mentioned above [19, 20, 21, 22, 23].

Identifying departure from universality in SUSY signals is important at more than one levels [24, 25, 26, 27, 28]. First, one would like to know whether or not the gaugino mass relation corresponding to a particular GUT representation is involved. The absence of any such obvious relation, however, still keeps SUSY GUT's alive, if the analysis of signals reveals that a linear combination of GUT multiplets is involved. It is only the decisive failure of such a finer analysis that can rule out a framework based on GUT. Therefore, if SUSY signals in some channel(s) are indeed seen at the LHC, the exercise of tracing them back to some underlying GUT framework, be it with gaugino mass universality or not, is of utmost importance.

Testing gaugino non-universality at the LHC, however, is not easy, especially if the ambitious task of looking for higher GUT representations has to be undertaken. There has been some detailed analysis of events and kinematics for non-universal gaugino masses in the context of the Tevatron [29, 30, 31], with reference to SU(5). Some phenomenological studies have been performed on different types of signals at the LHC, too [32, 33, 34], but the systematic investigation that is required to link the departure from universality to GUT representations has not so far been carried out in detail.

In our study, different representations of SUSY SU(5) and SO(10) are considered. No specific SUGRA origin of scalar masses is assumed in the general analyses, and we deliberately (and perhaps artificially) adhere to degenerate squark and slepton masses at low

energy in each case. However, we also present side by side the consequences of a SUGRA scenario with universal scalar masses at high scale. In each case, we consider a comprehensive set of SUSY signals, such as *jets + \cancel{E}_T* , *same – sign* as well as *opposite – sign dileptons*, *one isolated lepton* and *trileptons* alongwith *jets + \cancel{E}_T* (so called multichannel analysis [35, 36]). After subjecting the calculated event rates for these different final states and for different parameter values to such cuts as to suppress the standard model (SM) backgrounds, we look at their various ratios. This reduces uncertainties due to jet energy resolution, jet energy scale, parton distribution functions and so on. It also ensures that the departure from gaugino universality, rather than the overall scale of superparticle masses, is the decisive factor. Thereafter, we compare these ratios with the corresponding cases with a universal gaugino mass. The squark and gluino masses are kept at the same values during this comparison, since the most important cascades are dictated by them, and their masses can be approximately found out from the LHC data from \cancel{E}_T and effective mass distributions. Although we confine ourselves to a relatively rudimentary analysis, it is expected that more elaborate ones can be built on it following the same strategy. It is our belief that such an approach will mean full utilization of the LHC data in following up on any signature of SUSY, an exercise that is eminently appropriate at the present juncture [37].

In section 2, we briefly review the process by which non-universality arises at the GUT scale, and summarise the high-scale mass relations of gauginos in different GUT representations responsible for the non-universality. The strategy adopted in selecting the relevant SUSY parameters, and the event selection criteria for LHC, are outlined in section 3. The analysis of predicted signals for SU(5) and SO(10) are presented in sections 4.1 and 4.2, respectively. We summarise and conclude in section 5. Appendix A contains the various chargino and neutralino masses for different scenarios, while the absolute values of event rates in different channels (which has been found to be necessary supplements to the various ratios presented in the main text) are listed in Appendix B.

2 Non-universal SUSY GUT and gaugino mass ratios

In this section we review the issues that govern non-universality of supersymmetry breaking gaugino masses, arising under the influence of various GUT representations responsible for the SUSY breaking terms.

We adhere to a scenario where all soft SUSY breaking effects arise via hidden sector interactions in an underlying supergravity (SUGRA) framework. Specifically, we are considering

supersymmetric SU(5) and SO(10) gauge theories with an arbitrary chiral matter superfield content coupled to N=1 supergravity. The essential theoretical principles governing high-scale non-universality in gaugino masses as well as in gauge couplings have been discussed in a number of earlier works in the context of both SU(5) [19, 20] and SO(10) [21] gauge groups respectively. Later works that addressed the related phenomenology (mostly in the context of SU(5)) are by and large based on these principles [22, 23, 29, 30].

All gauge and matter terms including gaugino masses in the N=1 supergravity lagrangian depend crucially on two fundamental functions of chiral superfields. One of them is the gauge kinetic function $f_{\alpha\beta}(\Phi)$ which is an analytic function of the left-chiral superfields Φ_i . It transforms as a symmetric product of the adjoint representation as gauge superfields belong to the adjoint representation of the underlying gauge group (α, β being the gauge generator indices). The other is the real function $G(\Phi_i, \Phi_i^*)$ with $G = K + \ln|W|$ where K is the Kähler potential and W is the superpotential. G is a real function of the chiral superfields Φ_i and is a gauge singlet. However, $f_{\alpha\beta}$ in general has a non-trivial gauge transformation property. Based on whether its functional dependence on the chiral superfields involves singlet or non-singlet irreducible representations of the underlying gauge group, one has universal or non-universal gaugino masses at the GUT scale, when SUSY is broken.

In the component field notation, the part of the N=1 supergravity lagrangian containing kinetic energy and mass terms for gauginos and gauge bosons (including only terms containing the real part of $f(\Phi)$) reads [23]

$$e^{-1}\mathcal{L} = -\frac{1}{4}Re f_{\alpha\beta}(\phi)(-1/2\bar{\lambda}^\alpha \not{D}\lambda^\beta) - \frac{1}{4}Re f_{\alpha\beta}(\phi)F_{\mu\nu}^\alpha F^{\beta\mu\nu} + \frac{1}{4}e^{-G/2}G^i((G^{-1})_i^j)[\partial f_{\alpha\beta}^*(\phi^*)/\partial\phi^{*j}]\lambda^\alpha\lambda^\beta + h.c \quad (1)$$

where $G^i = \partial G/\partial\phi_i$ and $(G^{-1})_j^i$ is the inverse matrix of $G^j_i \equiv \partial G/\partial\phi^{*i}\partial\phi_j$, λ^α is the gaugino field, and ϕ is the scalar component of the chiral superfield Φ . The F -component of Φ enters the last term to generate gaugino masses. Thus, following equation (1), the lagrangian can be expressed as [30]

$$e^{-1}\mathcal{L} = -\frac{1}{4}Re f_{\alpha\beta}(\phi)(-1/2\bar{\lambda}^\alpha \not{D}\lambda^\beta) - \frac{1}{4}Re f_{\alpha\beta}(\phi)F_{\mu\nu}^\alpha F^{\beta\mu\nu} + \frac{F_{\dot{\alpha}\dot{\beta}}^j}{2}[\partial f_{\alpha\beta}^*(\phi^{*j})/\partial\phi^{*\dot{\alpha}\dot{\beta}}]\lambda^\alpha\lambda^\beta + h.c \quad (2)$$

where

$$F_{\dot{\alpha}\dot{\beta}}^j = \frac{1}{2}e^{-G/2}[G^i((G^{-1})_i^j)]_{\dot{\alpha}\dot{\beta}} \quad (3)$$

The Φ^j s can be classified into two categories: a set of GUT singlet supermultiplets Φ^S , and a set of non-singlet ones Φ^N . The non-trivial gauge kinetic function $f_{\alpha\beta}(\Phi^j)$ can be expanded in terms of the non-singlet components in the following way [19, 20, 30]:

$$f_{\alpha\beta}(\Phi^j) = f_0(\Phi^S)\delta_{\alpha\beta} + \sum_N \xi_N(\Phi^S) \frac{\Phi^N_{\alpha\beta}}{M} + \mathcal{O}\left(\frac{\Phi^N}{M}\right)^2 \quad (4)$$

where f_0 and ξ^N are functions of chiral singlet superfields, and M is the reduced Planck mass = $M_{Pl}/\sqrt{8\pi}$.

In principle, the gauge kinetic function $f_{\alpha\beta}$ is a function of all chiral superfields Φ^j . However, those which contribute significantly at the minimum of the potential by acquiring large vacuum expectation values (vev) are (i) gauge singlet fields which are part of the hidden sector (i.e. the fields Φ^S), and (ii) fields associated with the spontaneous breakdown of the GUT group to $SU(3) \times SU(2) \times U(1)$ (i.e. the fields Φ^N) [19, 20]. In equation (3), the contribution to the gauge kinetic function from Φ^N has to come through symmetric products of the adjoint representation of associated GUT group, since $f_{\alpha\beta}$ on the left side of (3) has such transformation property. Thus $f_{\alpha\beta}$ can have the ‘non-trivial’ contribution of the second type of terms only if one has chiral superfields belonging to representations which can arise from the symmetric products of two adjoint representations [22]. For SU(5), for example, one can have contributions to $f_{\alpha\beta}$ from all possible non-singlet irreducible representations to which Φ^N can belong :

$$(24 \times 24)_{symm} = 1 + 24 + 75 + 200$$

For SO(10), the possible representations are :

$$(45 \times 45)_{symm} = 1 + 54 + 210 + 770$$

The contribution to $f_{\alpha\beta}$ can also come from any linear combination of the singlet and possible non-singlet representations (as shown above) in case of both SU(5) and SO(10). It is now almost clear from (2) that these non-singlet representations can be responsible for non-universal gaugino mass terms at the GUT scale.

In order to obtain the low energy effective theory, we replace the fields Φ^S and Φ^N in the gauge kinetic term (3) by their vev’s and get $\langle f_{\alpha\beta} \rangle$. The value of $\langle f_{\alpha\beta} \rangle$ which determines the gaugino mass matrix crucially depends on the specific representation (or their linear combinations) responsible for the process [19, 20]. It is important to note here that, in this analysis, the breakdown of the symmetry from SU(5) to the SM gauge group has been assumed to take place at the GUT scale (M_X) itself. When there is an intermediate gauge

group H (as is possible for $SO(10)$), the vev of the gauge kinetic function depends not only on the chosen non-singlet representation but also crucially on the intermediate group H in the breaking chain [21]. In addition, the presence of intermediate scale can also affect the vev of the gauge kinetic function and hence gaugino mass ratios at the GUT scale [21].

Next, the kinetic energy terms are restored to the canonical form by rescaling the gauge superfields, by defining

$$F^\alpha_{\mu\nu} \rightarrow \hat{F}^\alpha_{\mu\nu} = \langle \text{Re} f_{\alpha\beta} \rangle^{\frac{1}{2}} F^\beta_{\mu\nu} \quad (5)$$

and

$$\lambda^\alpha \rightarrow \hat{\lambda}^\alpha = \langle \text{Re} f_{\alpha\beta} \rangle^{\frac{1}{2}} \lambda^\beta \quad (6)$$

Simultaneously, the gauge couplings are also rescaled (as a result of (4)):

$$g_\alpha(M_X) \langle \text{Re} f_{\alpha\beta} \rangle^{\frac{1}{2}} \delta_{\alpha\beta} = g_c(M_X) \quad (7)$$

where g_c is the universal coupling constant at the GUT scale. This shows clearly that the first consequence of a non-trivial gauge kinetic function is non-universality of the gauge couplings g_α at the GUT scale, if $\langle f_{\alpha\beta} \rangle$ carries a gauge index.

Once SUSY is broken by non-zero vev's of the F components of hidden sector chiral superfields, the coefficient of the last term in equation(2) is replaced by [19, 20, 30]

$$\langle F_{\alpha\beta}{}^i \rangle = \mathcal{O}(m_{\frac{3}{2}} M) \quad (8)$$

where $m_{\frac{3}{2}} = \exp(-\frac{\langle G \rangle}{2})$ is the gravitino mass. Taking into account the rescaling of the gaugino fields (as stated earlier in equation (4) and (5)) in equation (6), the gaugino mass matrix can be written down as in [30] or [19, 22]

$$M_\alpha(M_X) \delta_{\alpha\beta} = \sum_i \frac{\langle F_{\dot{\alpha}\dot{\beta}}^i \rangle}{2} \frac{\langle \partial f_{\alpha\beta}(\phi^{*i}) / \partial \phi^{*i}{}_{\dot{\alpha}\dot{\beta}} \rangle}{\langle \text{Re} f_{\alpha\beta} \rangle} \quad (9)$$

or

$$M_\alpha(M_X) \delta_{\alpha\beta} = \frac{1}{4} e^{-G/2} G^i ((G^{-1})^j{}_i) \frac{\langle \partial f_{\alpha\beta}^*(\phi^*) / \partial \phi^{*j} \rangle}{\langle \text{Re} f_{\alpha\beta} \rangle} \quad (10)$$

which demonstrates that the gaugino masses are non-universal at the GUT scale. The underlying reason for this is the fact that $\langle f_{\alpha\beta} \rangle$ can be shown to acquire the form $f_\alpha \delta_{\alpha\beta}$ [19, 20], thanks to the symmetric character of the representations. Consequently, the derivatives on the right-hand side of the above equations acquire such forms as to render M_α non-universal in the gauge indices. On the contrary, if symmetry breaking occurs via gauge singlet fields only, one has $f_{\alpha\beta} = f_0 \delta_{\alpha\beta}$ from equation (4) and as a result, $\langle f_{\alpha\beta} \rangle = f_0$. Thus both

gaugino masses and the gauge couplings are unified at the GUT scale, as can be seen from equations (7) and (10).

Following the approach in [19, 20, 22, 30], we make a further simplification by neglecting the non-universal contributions to the gauge couplings at the GUT scale. The gaugino mass ratios at high scale thus obtained [19, 21] are shown in Tables 1 and 2. We also present the approximate values of the ratios at the Electroweak Symmetry Breaking scale (EWSB) in those tables. While the effects corresponding to all symmetric representations of SU(5) have been shown, we have presented the case for only the lowest representation of SO(10). This is because, SO(10) being a rank-5 gauge group, the low-energy consequences of the mass ratios depend on not only the specific breaking chain adopted, but also the presence (or otherwise) and magnitudes of intermediate breaking scale. A proliferation of such features affects the collider phenomenology in too complicated a manner to be related easily to high scale physics. Therefore, we illustrate our points by taking the lowest relevant representation, and using the mass ratios corresponding to two breaking chains, assuming that the breakdown to $SU(3) \times SU(2) \times U(1)$ takes place at the GUT scale itself in each case.

Table 1: High-scale and approximate low-scale gaugino mass ratios for SU(5).

Representation	$M_3 : M_2 : M_1$ at M_{GUT}	$M_3 : M_2 : M_1$ at M_{EWSB}
1	1:1:1	6:2:1
24	2:(-3):(-1)	12:(-6):(-1)
75	1:3:(-5)	6:6:(-5)
200	1:2:10	6:4:10

Table 2: High-scale and approximate low-scale gaugino mass ratios for SO(10).

Representation	$M_3 : M_2 : M_1$ at M_{GUT}	$M_3 : M_2 : M_1$ at M_{EWSB}
1	1:1:1	6:2:1
54(i): $H \rightarrow SU(2) \times SO(7)$	1:(-7/3):1	7:(-5):1
54(ii): $H \rightarrow SU(4) \times SU(2) \times SU(2)$	1:(-3/2):(-1)	7:(-3):(-1)

3 SUSY signals and backgrounds: strategy for analysis

In this section we discuss and analyse the difference in the collider signature due to non-universal gaugino masses at the GUT scale for various non-singlet representations of SU(5)

and SO(10) GUT group in the context of the LHC.

3.1 Choice of SUSY parameters

In our analysis we have confined ourselves to R -parity conserving supersymmetry where the lightest neutralino is the LSP. Thus all SUSY signals at the LHC are characterized by a large amount of missing E_T carried by the LSP, together with jets and/or leptons of various multiplicity.

A large part of our analysis is done for a scenario where the gaugino masses are obtained through one-loop running from the non-universal mass parameters at the high scale, whereas the low-energy scalar masses are all treated as phenomenological inputs. Furthermore, since we wish to examine the effects of gaugino non-universality in isolation, we have taken all the squark and slepton masses to be degenerate. This not only avoids special situations arising from SUSY cascade decays due to a spread in the sfermion masses, but also keeps the scenario above board by suppressing flavour-changing neutral currents (FCNC) [38]. The Higgsino mass parameter μ , too, is a free parameter here. The mass parameters of the Higgs sector are determined once μ , the neutral pseudoscalar mass (m_A) and $\tan\beta$ (the ratio of the two Higgs vev's) are specified.

Side by side, we also present an analysis pertaining to a non-universal SUGRA scenario where the low energy supersymmetric spectrum is generated from a common scalar mass m_0 , common trilinear coupling A_0 and $sgn(\mu)$, with non-universal gaugino masses M_i at high scale arising from various non-singlet representations of SU(5) and SO(10). While this allows a spread in the low-energy sfermion masses, it also gives one the opportunity to compare the predicted collider results with those in the phenomenological scalar spectrum mentioned above. It has been made sure that in both this case and the previous one, the parameter choices are consistent with the LEP bounds, as far as the neutral Higgs mass, the lighter chargino mass etc. are concerned [39].

The spectrum in the first case is generated by the option **pMSSM** in the code **SuSpect** v2.3 [40]. It should be remembered that our goal here is to generate a phenomenological low-energy spectrum with degenerate scalar masses, but with the three gaugino mass parameters related not by high-scale universality but by the specific conditions answering to various non-singlet GUT representations. In order to implement this, we resort to a two-step process. The first step is to give as inputs non-universal gaugino masses at the GUT scale, and evolve them down to low scale through one-loop renormalization group equations (which do not involve scalar masses). This yields a phenomenological gaugino spectrum which, to a

reasonable approximation, corresponds to the specific non-singlet GUT representation under scrutiny. In the second step, we feed the thus obtained gaugino masses, together with the degenerate scalar masses (and the free parameters in the Higgs sector) at the electroweak symmetry breaking (EWSB) scale, into **SuSpect** as low energy inputs in the **pMSSM** option. The subsequent running of **SuSpect** yields a low-energy spectrum which is basically phenomenological, but ensures gauge coupling unification at high scale (see discussion in the previous section), and is nonetheless consistent with laboratory constraints on a SUSY scenario. We have used the low-energy value of $\alpha_3(M_Z)^{\overline{MS}} = 0.1172$ for this calculation which is default in **SuSpect**. Throughout the analysis we have assumed the top quark mass to be 171.4 GeV. Electroweak symmetry breaking at the ‘default scale’ $\sqrt{m_{\tilde{t}_L} m_{\tilde{t}_R}}$ has been ensured in this procedure, together with the requirement of no tachyonic modes for sfermions. No radiative correction to gaugino masses has been considered, which does not affect the main flow of our analysis in any significant way. Full one-loop and the dominant two-loop corrections to the Higgs masses are incorporated. And finally, consistency with low-energy constraints $b \rightarrow s\gamma$ and muon anomalous magnetic moment are checked for every combination of parameters used in the analysis. Preferring to be strictly confined to accelerator signals, we have not considered dark matter constraints in our analysis. For studies in this direction, we refer the reader to [22, 41, 42, 43] where the issues related to dark matter in non-universal gaugino scenarios have been discussed. It should also be remembered that, although we shall henceforth refer to this case as **pMSSM** for convenience, the low-energy spectrum is not purely ‘phenomenological’, since the gaugino masses at low energy actually correspond to specific high-scale GUT-breaking conditions.

We attempt a representative analysis of the above situation by taking all possible combinations of parameters, arising out of the following choices, for each type of GUT breaking scheme:

$$m_{\tilde{g}} = [500 \text{ GeV}, 1000 \text{ GeV}, 1500 \text{ GeV}]$$

$$m_{\tilde{f}} = [500 \text{ GeV}, 1000 \text{ GeV}]$$

$$\mu = [300 \text{ GeV}, 1000 \text{ GeV}]$$

$$\tan \beta = [5, 40]$$

where by $m_{\tilde{f}}$ we denote all the degenerate squark and slepton masses. This gives us a total of 24 combinations which include the most important kinematics regions in terms of $m_{\tilde{g}}$ and $m_{\tilde{q}}$ namely, (i) $m_{\tilde{g}} \gg m_{\tilde{f}}$, (ii) $m_{\tilde{q}} \gg m_{\tilde{g}}$ and (iii) $m_{\tilde{q}} \simeq m_{\tilde{g}}$ which crucially controls the final state scenario at the collider. Also the variation in μ changes the chargino and neutralino compositions which affect the various decay branching fractions involved in the cascades.

We have also taken two values of $\tan\beta$, one close to the limit coming from $e^+ e^-$ collider data, and the other on the high side, since they also control the chargino-neutralino sector. For all these points we keep all the trilinear coupling constants $A_0=0$ and the pseudoscalar Higgs mass $m_A=1000$ GeV.

For studying the other scenario, namely, gaugino mass non-universality in a **SUGRA** setting, the spectrum is generated with the help of **ISASUGRA v7.75** [44]. As mentioned earlier, here one uses as the inputs a common scalar mass m_0 , a common trilinear coupling A_0 , $\tan\beta$ and $sgn(\mu)$, along with non-universal gaugino masses m_i at the GUT scale (with ratios as appropriate for various GUT-breaking representations) and run down to low scale via two-loop renormalization group equations. The chargino and neutralino spectra are given in Table A9, Appendix A. We select a smaller number of samples than in the case of **pMSSM**, taking $A_0=0$, $sgn(\mu)$ as positive and $\tan\beta=5$. We choose m_0 at the GUT scale such that, for $m_{\tilde{g}}=1000$ GeV at the low scale, the first two generations of squark masses are clubbed around 1000 GeV. We know that the scalar mass thus obtained at the electroweak symmetry breaking scale with a high scale input by renormalisation group equation (RGE) has almost 90 % contribution from gauginos due to the running [45]. This value turns out to be 506 GeV at the GUT scale. As is done earlier, we tune the SU(3) gaugino mass M_3 at the high scale to get $m_{\tilde{g}}=500$ GeV, 1000 GeV and 1500 GeV. We stick to $m_0=506$ GeV at the GUT scale for all these cases. The low-energy spectrum is consistent with radiative electroweak symmetry breaking as well as all other phenomenological constraints [46].

3.2 Collider simulation

The spectra generated as described in the previous section are fed into the event generator **Pythia 6.405** [47] by **SLHA** interface [48] for the simulation of pp collision with centre of mass energy 14 TeV.

We have used **CTEQ5L** [49] parton distribution functions, the QCD renormalisation and factorisation scales being both set at the subprocess centre-of-mass energy $\sqrt{\hat{s}}$. All possible SUSY processes and decay chains have been kept open. In the illustrative study presented here, we have switched off initial and final state radiation as well as multiple interactions. However, we take hadronisation into account using the fragmentation functions inbuilt in **Pythia**. We have checked our analysis code against earlier studies done at the parton level in the MSSM framework [7]. We also checked our code in the context of Tevatron using [50]. We checked all the cross-sections with **CalCHEP** also [51].

The standard final states in connection with R -parity conserving SUSY have been looked

for. All of these have been discussed in the literature in different contexts [7, 11, 29, 52]. These are

- Opposite sign dilepton (OSD) : $(\ell^\pm\ell^\mp) + (\geq 2) jets + E_T$
- Same sign dilepton (SSD) : $(\ell^\pm\ell^\pm) + (\geq 2) jets + E_T$
- Single lepton ($(1\ell + jets)$): $1\ell + (\geq 2) jets + E_T$
- Trilepton ($(3\ell + jets)$): $3\ell + (\geq 2) jets + E_T$
- Inclusive jet ($jets$): $(\geq 3) jets + E_T$

where ℓ stands for electrons or muons. The cuts used are as follows:

- Missing transverse momentum $E_T \geq 100$ GeV.
- $p_{T\ell} \geq 20$ GeV and $|\eta_\ell| \leq 2.5$ [7].
- An isolated lepton should have lepton-lepton separation $\Delta R_{\ell\ell} \geq 0.2$, lepton-jet separation $\Delta R_{\ell j} \geq 0.4$, the energy deposit due to jet activity around a lepton E_T within $\Delta R \leq 0.2$ of the lepton axis should be ≤ 10 GeV.
- $E_{Tjet} \geq 100$ GeV and $|\eta_{jet}| \leq 2.5$ [7].

where $\Delta R = \sqrt{\Delta\eta^2 + \Delta\phi^2}$ is the separation in pseudorapidity and azimuthal angle plane.

Jets are formed in `Pythia` using `PYCELL` jet formation criteria with $|\eta_{jet}| \leq 5.0$ in the calorimeter, $N_{\eta_{bin}} = 100$ and $N_{\phi_{bin}} = 64$. For a partonic jet to be considered as a jet initiator $E_T > 2$ GeV is required while a cluster of partonic jets to be called a hadron-jet $\sum_{parton} E_{Tjet}$ is required to be more than 20 GeV. For a formed jet the maximum ΔR from the jet initiator is 0.4.

3.3 Backgrounds

We have generated all dominant standard model (SM) events in `Pythia` for the same final states, using the same factorisation scale, parton distributions and cuts. It has been found that $t\bar{t}$ production gives the most serious backgrounds in all channels excepting in the trilepton channel, for which the electroweak backgrounds are rather effectively removed by our event selection criteria.

The signal and background events have been all calculated for an integrated luminosity of 300 fb^{-1} . As has been already mentioned, the ratios of events in the different final states have been presented, which presumably reduces some uncertainties in prediction. Cases where the number of signal events in any of the channels used in the ratio(s) is less than three have been left out. Also, in the histograms (to be discussed in the next section), cases where any of the entries in the ratio has $\sigma = S/\sqrt{B} \leq 2$ (S, B being the number of signal and background events) have been specially marked with a '#', since our observations on them may become useful if statistics can be improved.

4 Prediction for different GUT representations

4.1 Non-universal SU(5)

We discuss here the possibility of interpreting non-universality arising in various SU(5) representations, namely **24**, **75**, **200**, and compare them with the universal case. For the **pMSSM** kind of framework, and adhering to the approach outlined already, we present in figures 1 - 8 the ratios of the various types of signals for each of the above schemes of non-universality. Figure 9 contains our prediction for SU(5) SUGRA. We have taken the ratio of the number of each type of signal event to the number of OSD events at the corresponding point in the parameter space. Thus each panel shows four ratios, namely, SSD/OSD , $(1\ell + jets)/\text{OSD}$, $(3\ell + jets)/\text{OSD}$ and $jets/\text{OSD}$ in the form of histograms. For reasons already mentioned, the ratio space is a rather reliable discriminator in the signature space. However, as we shall see, there are regions where all the ratios turn out to be of similar values for different GUT representations. In order to address such cases and make the presentation complete, we also present the absolute values of the cross-sections for each type of signal in Appendix B, while the chargino and neutralino spectra in different cases are found in Appendix A.

We plot a particular ratio (eg. SSD/OSD) along the y-axis for all non-singlet representations along with the universal one at three gluino masses 500 GeV, 1000 GeV and 1500 GeV in the x-axis with fixed sfermion mass $m_{\tilde{f}}$, μ and $\tan\beta$. We club all the different ratio plots in one pannel and discuss the outcome as a whole.

It can perhaps be assumed that, if SUSY signals are seen at the LHC, their kinematic distributions in variables such as p_T or effective mass will yield some useful information about the range of the gluino and sfermion masses. Adding to this the information extracted from the Higgs sector, one may be in a position to examine the aforementioned ratios, and compare

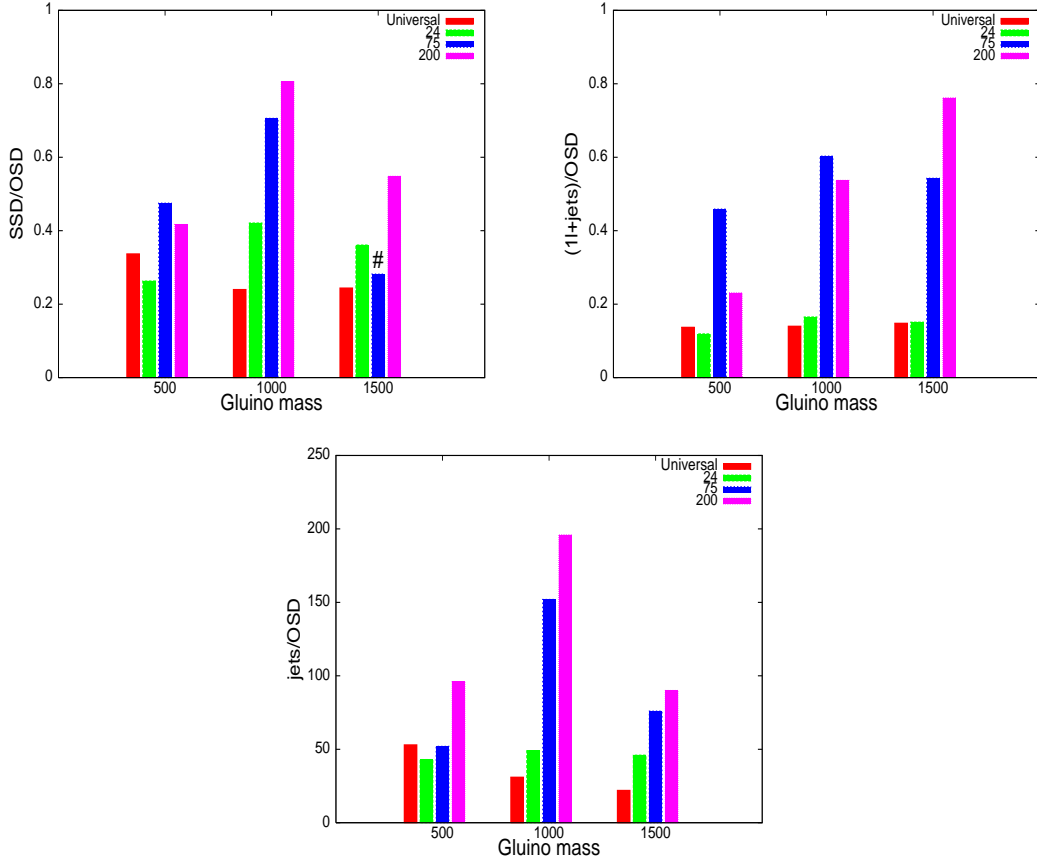


Figure 1: Event ratios for pMSSM in SU(5): $m_{\tilde{f}} = 500$ GeV, $\mu = 300$ GeV, $\tan \beta = 5$

them with our sample results.

In general, the wide multiplicity of parameters makes the variation of different rates with GUT representations far from transparent. However, a few features are broadly noticeable from figures 1 - 8, and we list them below, before giving a brief account of each individual figure.

1. The event ratios for the representations **75** and **200** are mostly bigger than those for **24** and the universal case. These correspond to the cases where the chargino and neutralino masses are relatively large compared to the gluino mass, which in turn is an artifact of larger M_1 and M_2 compared to M_3 at the GUT scale. The two worst sufferers due to this are the OSD and SSD events; of which the former suffers more. This is due to the different masses and compositions of χ_2^0 and χ_1^\pm (see next para), which are principally responsible for the OSD and SSD events respectively. The ratios

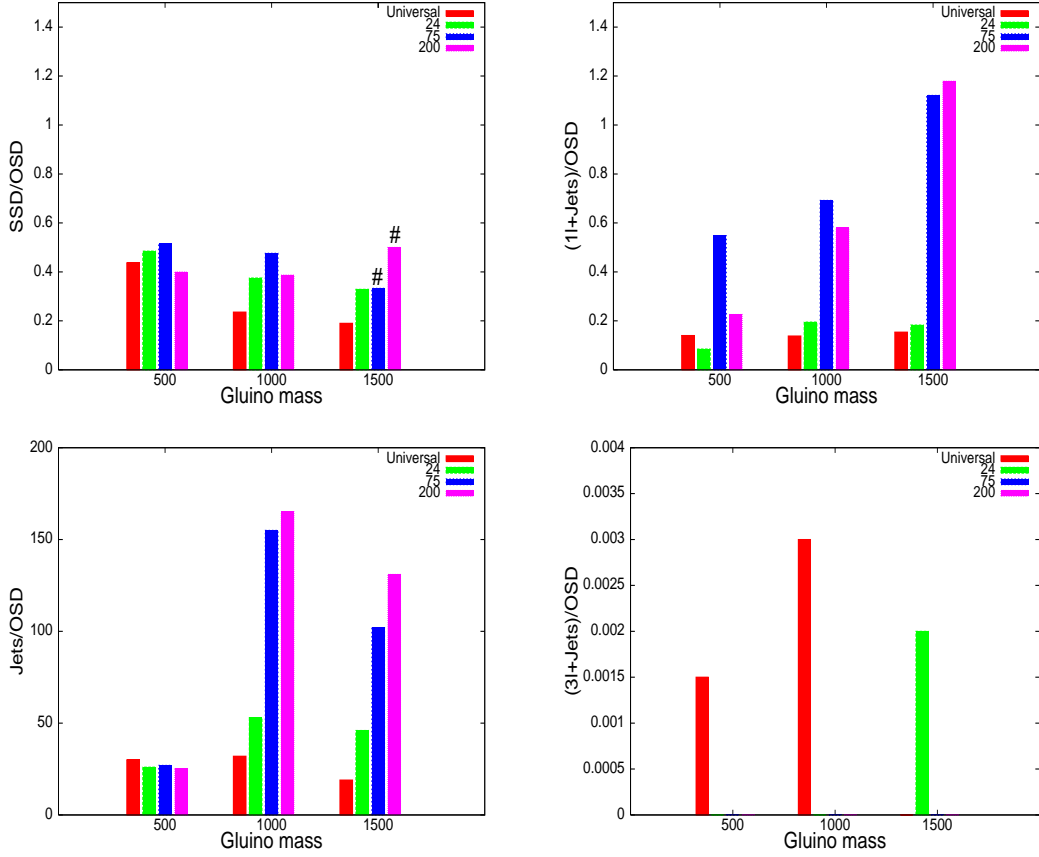


Figure 2: Event ratios for **pMSSM** in **SU(5)**: $m_{\tilde{f}}=500$ GeV, $\mu=300$ GeV, $\tan\beta=40$

for **200** are also separable from the others in at least one channel for a large number of cases. In contrast, **24** and the universal case often behave similarly in the SSD/OSD , $(1l+jets)/OSD$ and $jets/OSD$ ratios. While this indicates a partially available handle for discrimination over a substantial region of the parameter space, distinction between **24** and the universal case is possible relatively easily through absolute values of the event rates. However, in cases where distinguishing **75** and **200** from the ratios are difficult, distinction from absolute number of events are more challenging, because of the rather low rates of events in such cases.

2. In general, the $(3l+jets)$ channel is a rather useful discriminator. This is because in the non-universal cases, especially for **75** and **200**, the masses of χ_2^0 and χ_1^\pm are rather widely spaced, as opposed to the case of universality. This can be attributed to the fact that the ratio M_2/M_1 is different from the universal case, and, while the gaugino

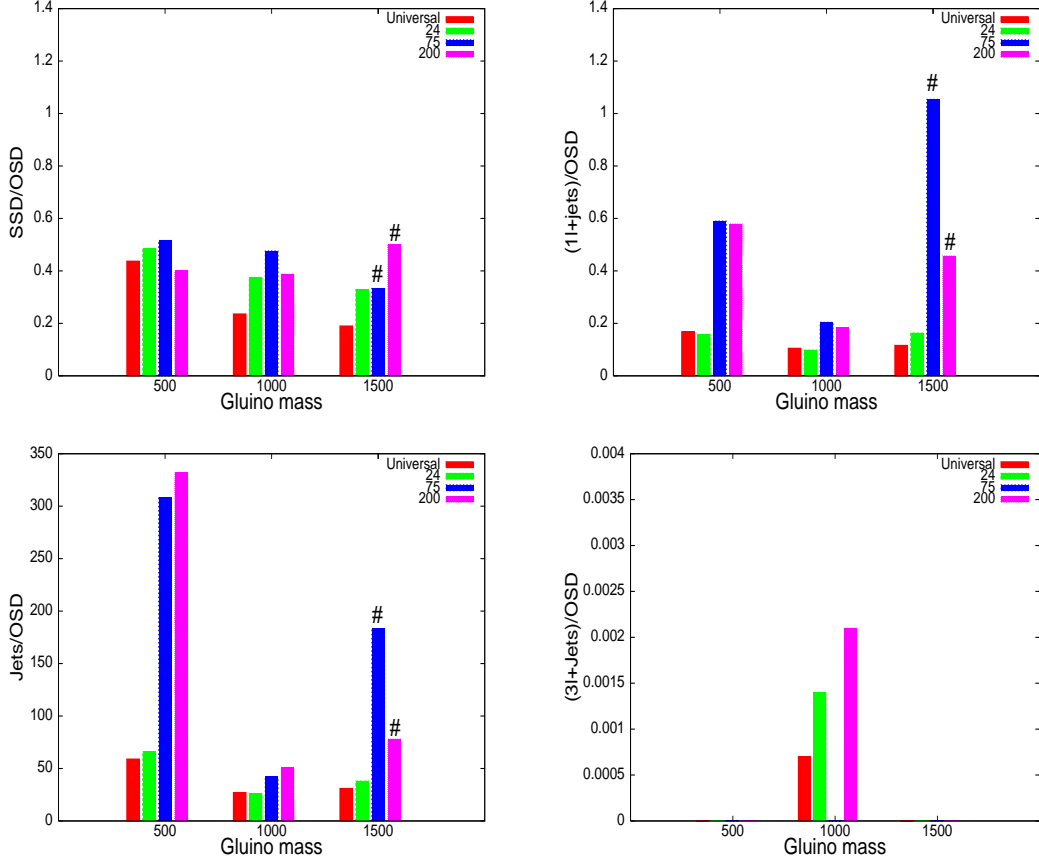


Figure 3: Event ratios for **pMSSM** in **SU(5)**: $m_{\tilde{f}} = 1000$ GeV, $\mu = 300$ GeV, $\tan \beta = 5$

contribution to χ_1^\pm comes exclusively from the Wino, χ_2^0 has Bino contributions as well with the altered mass ratios. For **24**, too, the spacing between χ_2^0 and χ_1^0 is different from the universal case. Thus the suppression of tripletons for **75** and **200** can be useful, while the maximum number of such events can be obtained in the universal case. All these affect the branching ratios for $\chi_2^0 \chi_1^\pm \rightarrow 3\ell + E_{\cancel{H}}$. However, events rates tend to be low in this channel, as a result of which its ratio with the OSD rates cannot be presented in a number of cases. However, the rates are in general on the higher side for $\tan \beta = 40$ than 5, because of the lower mass of the lighter sbottom state in the former case, which enhances its production and subsequent cascades to χ_1^\pm and χ_2^0 . Besides, the compositions of χ_1^\pm and χ_2^0 also is somewhat altered by a different $\tan \beta$.

- SSD/OSD is usually less useful in distinguishing among the different cases of non-universality. This is because the modified gaugino mass ratios at high scale due to

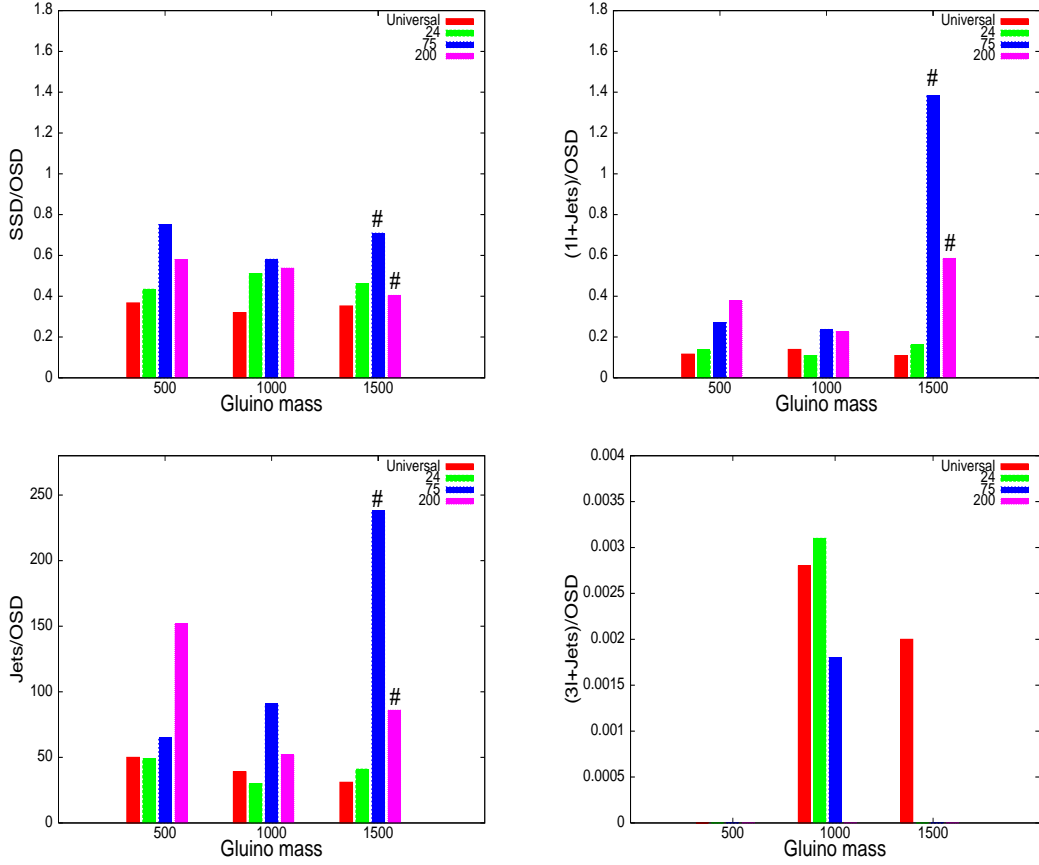


Figure 4: Event ratios for **pMSSM** in **SU(5)**: $m_{\tilde{f}} = 1000$ GeV, $\mu = 300$ GeV, $\tan \beta = 40$

non-singlet GUT-breaking representations usually tend to affect $m_{\chi_1^\pm}$ and $m_{\chi_2^0}$ similarly, thus having the same impact on both the SSD and OSD rates.

4. The rates for single lepton events, as in the case of trileptons, are affected significantly once the isolation cut between leptons and jets is turned on.
5. The absolute rates for events with jets in the final state are always way above the backgrounds with the cuts adopted here. However, the suppression of OSD, SSD and single-lepton channels for (a) high gluino/squark masses and (b) relatively higher chargino/neutralino masses for cases such as **75** and **200** often tend to drown them with backgrounds, as a result of which the ratios are likely to be useful only when statistics can be significantly improved. The trilepton events are rather easy to keep above backgrounds, due to the rather stiff jet p_T cut and the missing- E_T cut.

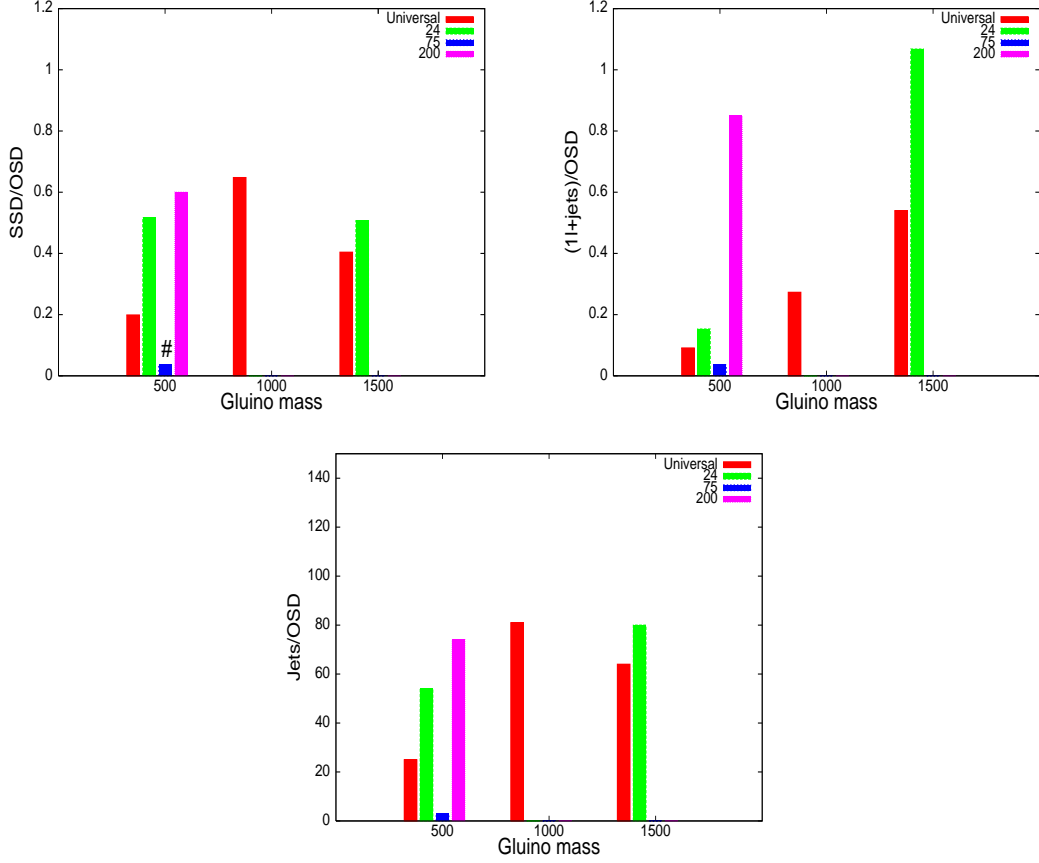


Figure 5: Event ratios for **pMSSM** in **SU(5)**: $m_{\tilde{f}}=500$ GeV, $\mu = 1000$ GeV, $\tan \beta = 5$

6. The SSD and single lepton events (and sometimes the OSD events) for $m_{\tilde{f}}=1000$ GeV, and gluino mass in the range of 1000 GeV or higher, are relatively background-prone for **75** and **200**. The reason for this is higher values of the chargino and neutralino masses and the suppression of leptonic final states by heavy sleptons.
7. For $\mu=1000$ GeV, $m_{\tilde{f}}=500$ GeV and $m_{\tilde{g}} \gg 500$ GeV, most of the non-universal scenarios give inconsistent spectrum, because both the gaugino and Higgsino components of the lightest neutralino tend to make it heavier than some sfermion(s). For $m_{\tilde{g}}=500$ GeV, too, this happens for $\tan \beta=40$, as it lowers the lighter stau mass below that of χ_1^0 .
8. For μ increased from 300 GeV to 1000 GeV in the universal case, particularly with gauginos on the lower side, the Higgsino component in the lighter charginos/neutralinos decreases and enhances the probability of leptons arising from cascades. Thus, say, the

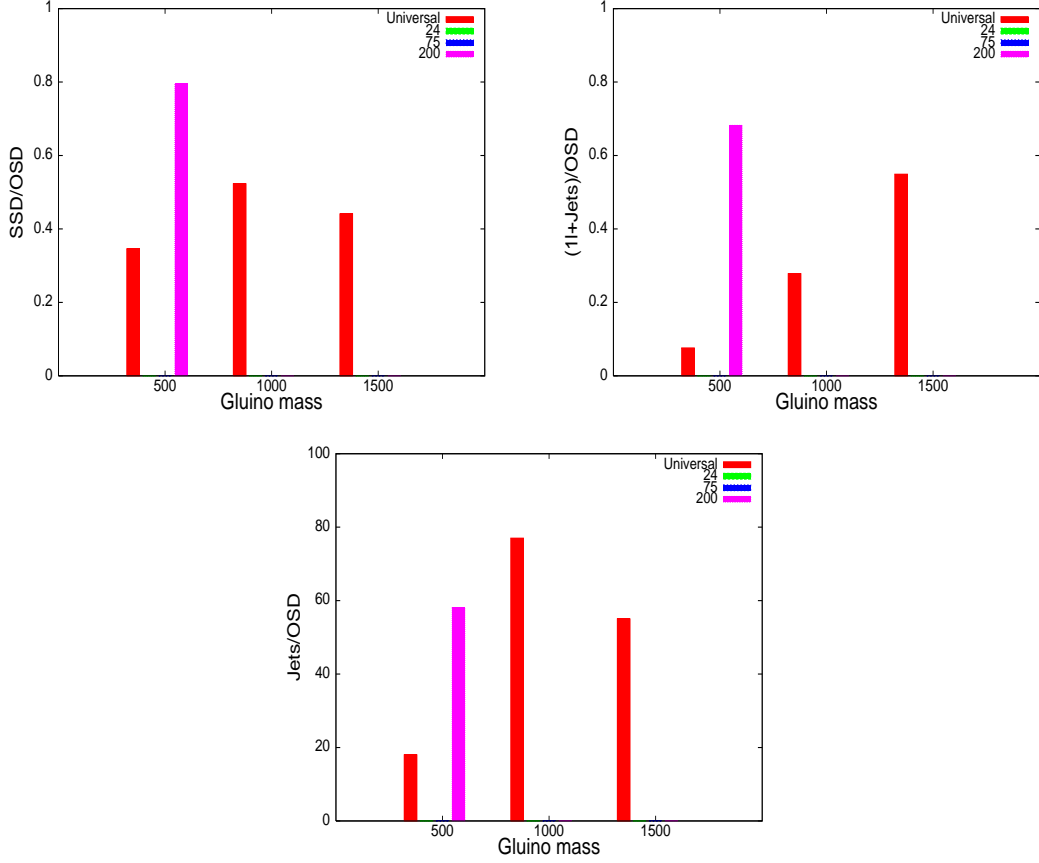


Figure 6: Event ratios for pMSSM in SU(5): $m_{\tilde{g}}=500$ GeV, $\mu=1000$ GeV, $\tan\beta=40$

ratio $jets/OSD$ is smaller for higher μ . This feature, however, is not always there (for example for non-universality, ostensibly due to the more complicated gaugino mass ratios as well as the different hierarchy between the gluino and chargino/neutralino masses).

- It should be noted (in the contexts of both SU(5) and SO(10)) that no observation is predicted in some channels for certain representations and in certain regions of the parameter space. Such ‘null observations’, however, can themselves be of use in distinguishing among scenarios.

In the region of the parameter space illustrated in figure 1, the $3\ell + jets$ channel search gives null result for all the representations. For $m_{\tilde{g}}=500$ GeV, one can distinguish the case of **75** from others from the ratio $(1\ell + jets)/OSD$, and **200** from $jets/OSD$. It is very difficult to distinguish the universal and **24** from any of the plots. However, as has been mentioned

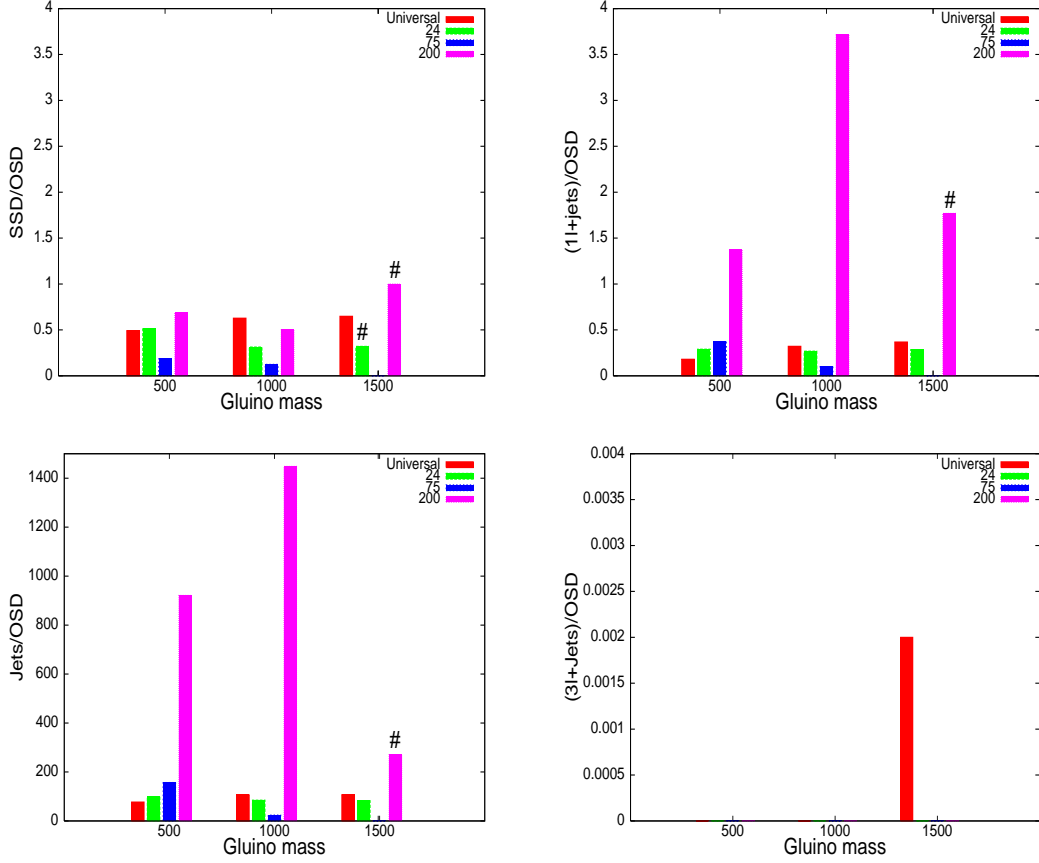


Figure 7: Event ratios for **pMSSM** in **SU(5)**: $m_{\tilde{g}}=1000$ GeV, $\mu=1000$ GeV, $\tan\beta=5$

already, one can do so from the absolute number in the OSD channel search where **24** gives a significantly larger number. For $m_{\tilde{g}}=1000$ GeV, the ratios for both **75** and **200** are distinctly larger than those for **24** and the universal case, when one considers SSD/OSD , $(1l+jets)/OSD$ and $jets/OSD$. However, distinguishing between **75** and **200** is difficult not only in this ratio space but also from the absolute rates. Distinction between the remaining two representation is possible through SSD/OSD and also through the absolute rates in the OSD channel, where the universal case gives sufficiently larger number than **24**. This is because the charginos and higher neutralinos become sufficiently heavy in the latter case. For $m_{\tilde{g}}=1500$ GeV, the leptonic signals corresponding to **75** are beset with backgrounds, thus putting the ratio SSD/OSD at the mercy of statistics. **200** can be separated through SSD/OSD or $(1l+jets)/OSD$, while **75** is distinguishable from **1** and **24** quite clearly with the help of $(1l+jets)/OSD$. However, the distinction between **24** and the universal case is

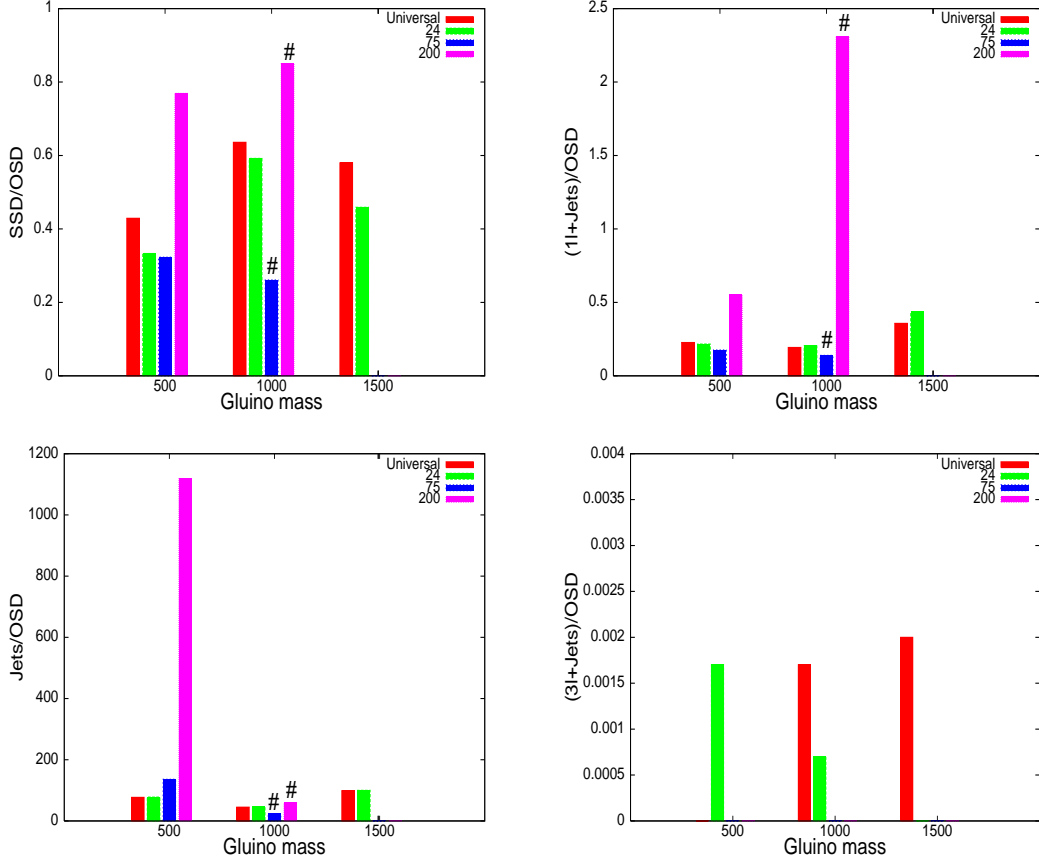


Figure 8: Event ratios for **pMSSM** in **SU(5)**: $m_{\tilde{g}}=1000$ GeV, $\mu=1000$ GeV, $\tan\beta=40$

still difficult. Figure 2 differs from the figure 1 only in $\tan\beta$, whose effect on $(3l+Jets)/OSD$ has already been discussed. The SSD/OSD values in this case shows a different behaviour from $\tan\beta=5$ for $m_{\tilde{g}}=1000$ GeV, the ratio showing a rather flat character with respect to gluino mass variation. Moreover, the ratio $(1l+jets)/OSD$ also shows a significant enhancement for **75**.

Figures 3 and 4 differ from figures 1 and 2 in terms of $m_{\tilde{g}}$ only. For $m_{\tilde{g}}=500$ GeV, the ratios $(1l+jets)/OSD$ and $jets/OSD$ for **75** and **200** are well separated from others for $\tan\beta=5$, while the distinction between these two representations from the ratios is difficult. For $\tan\beta=40$, however, SSD/OSD and $jets/OSD$ make such distinction possible. Similar conclusions can be drawn for higher gluino masses as well, except that the $(3l+jets)$ channel emerges as a successful discriminator for $m_{\tilde{g}}=1000$ GeV.

The predictions corresponding to a high value of μ are shown in figures 5 and 6. This

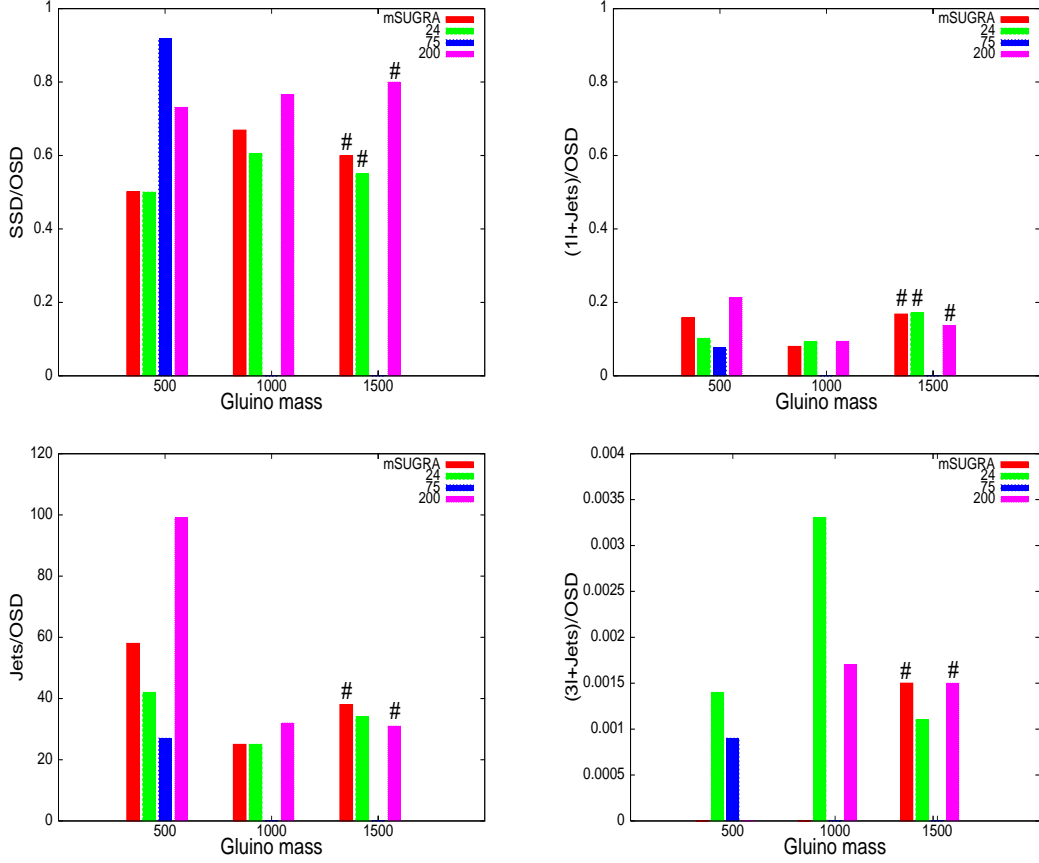


Figure 9: Event ratios for SU(5) **SUGRA** with non-universal gaugino masses: $m_0 = 506$ GeV, $\tan\beta = 5$, $sgn(\mu) = +$, $A_0 = 0$

scenario often does not allow a consistent spectrum except for a low gluino mass, because, with sfermion masses on the the low side, the lightest neutralino is mostly not the LSP. The situation is found to be worse for $\tan\beta = 40$. However, all the aforementioned ratios provide rather easy ways of discriminations among the different representations for those cases which survive.

Figures 7 and 8 show predictions with both the sfermion masses and μ at 1000 GeV. For both the values of $\tan\beta$, **200** is clearly differentiable, for cases where consistent spectra that can rise above the background are possible. While the ratio SSD/OSD can act as a fair discriminator for $\tan\beta = 40$, the *single-lepton* channel or *jets/OSD* do better for $\tan\beta = 5$. The signals for **24** and the universal case still require knowledge of the absolute event rates. For $\tan\beta = 40$, these two representations can be distinguished through $(3l + jets)/OSD$,

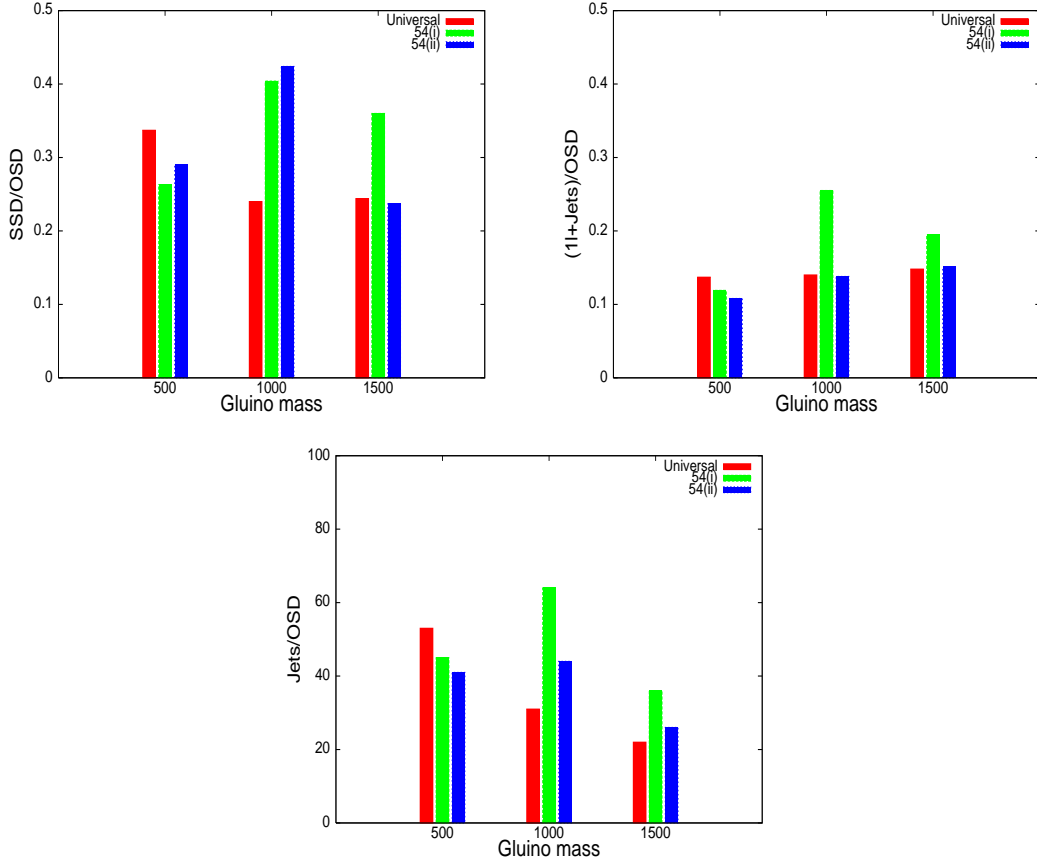


Figure 10: Event ratios for **pMSSM** in **SO(10)**: $m_{\tilde{f}} = 1000$ GeV, $\mu = 300$ GeV, $\tan \beta = 5$

which does not give sufficient event rates for the universal case for $m_{\tilde{g}} = 500$ GeV, while the same thing happens to **24** for $m_{\tilde{g}} = 1500$ GeV. Both of these cases yield measurable $(3l + jets)/OSD$ rates for $m_{\tilde{g}} = 1000$ GeV, but are sufficiently apart numerically.

Figure 9 contains some illustrative numbers for SUGRA with non-universal gaugino masses at high scale. It may be noted that, corresponding to $m_{\tilde{g}} = 1000$ GeV, the values of the lighter charginos/neutralinos become too small to be allowed by LEP results, whereas for $m_{\tilde{g}} = 1500$ GeV, no spectrum is generated for **75** since it cannot implement radiative electroweak symmetry breaking (the gaugino contributions being responsible for rendering all scalar mass-squared values positive). For $m_{\tilde{g}} = 500$ GeV, **75** is allowed, and can easily be distinguished from either the SSD/OSD or the $jets/OSD$ ratio. Identification of **200** is also possible through $jets/OSD$. **24** and **75** may be separated from **200** and the universal case with the help of the ratio $(3l + jets)/OSD$. On the whole, for gluino mass on the lower side, all the four GUT breaking schemes can be distinguished from each other through the

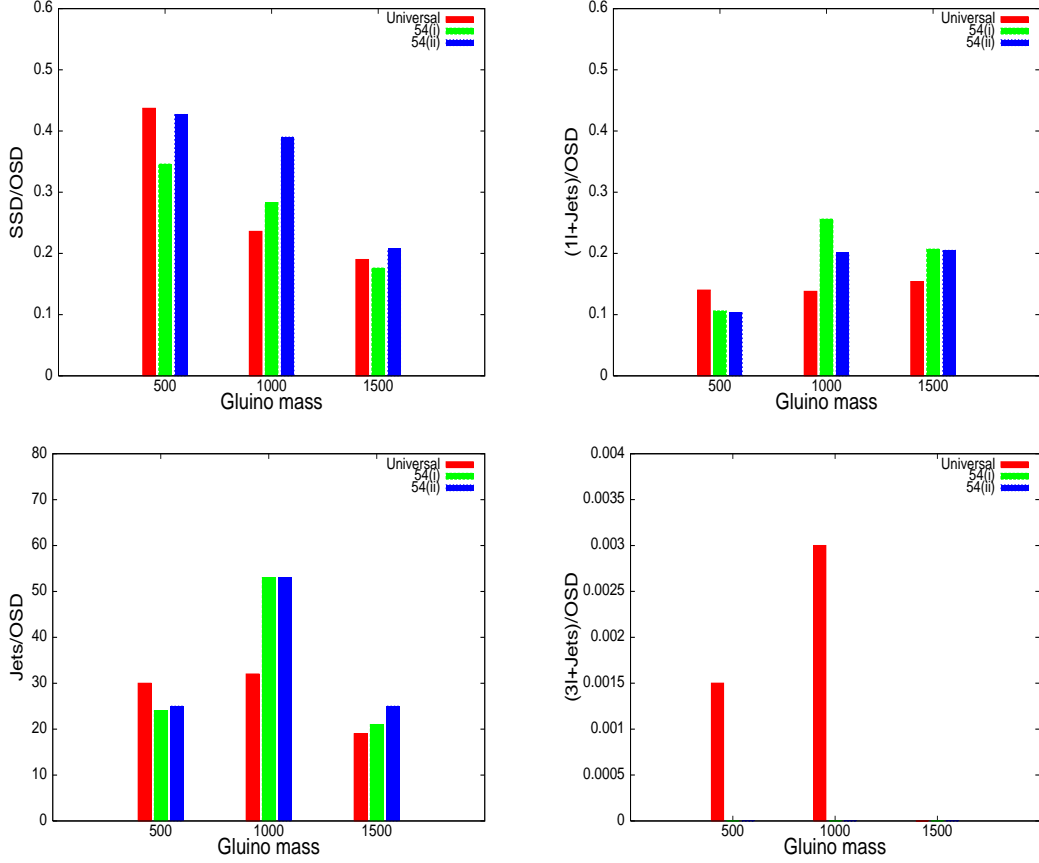


Figure 11: Event ratios **pMSSM** in **SO(10)**: $m_{\tilde{g}} = 500$ GeV, $\mu = 300$ GeV, $\tan\beta = 40$

ratios SSD/OSD , in conjunction with non-observation (or otherwise) of $(3\ell + jets)/\text{OSD}$. This is in a sense a gratifying conclusion, since the one can make useful inference even while avoiding the overall uncertainties of events containing jets only. $(1\ell + jets)/\text{OSD}$ is quite suppressed in all the cases and are numerically quite uniform, so that it is not of much help. For $m_{\tilde{g}} = 1000$ GeV, **24** and **200** can be separated quite visibly from $(3\ell + jets)/\text{OSD}$, while non-observation of $(3\ell + jets)$ events (with the other final states observed) will point towards **75** since **75** is inadmissible for the reason mentioned above and observations in all other channels indicate **24**. The results presented for $m_{\tilde{g}} = 1500$ GeV are not numerically very different from each other; however, for all representations excepting **24**, the OSD events do not rise beyond 2σ above the backgrounds for an integrated luminosity of 300 fb^{-1} . For **24**, all of the *jets*, OSD and *trilepton* channels rise above backgrounds, and thus the ratios jets/OSD and $(3\ell + jets)/\text{OSD}$ should be able to make it stand out.

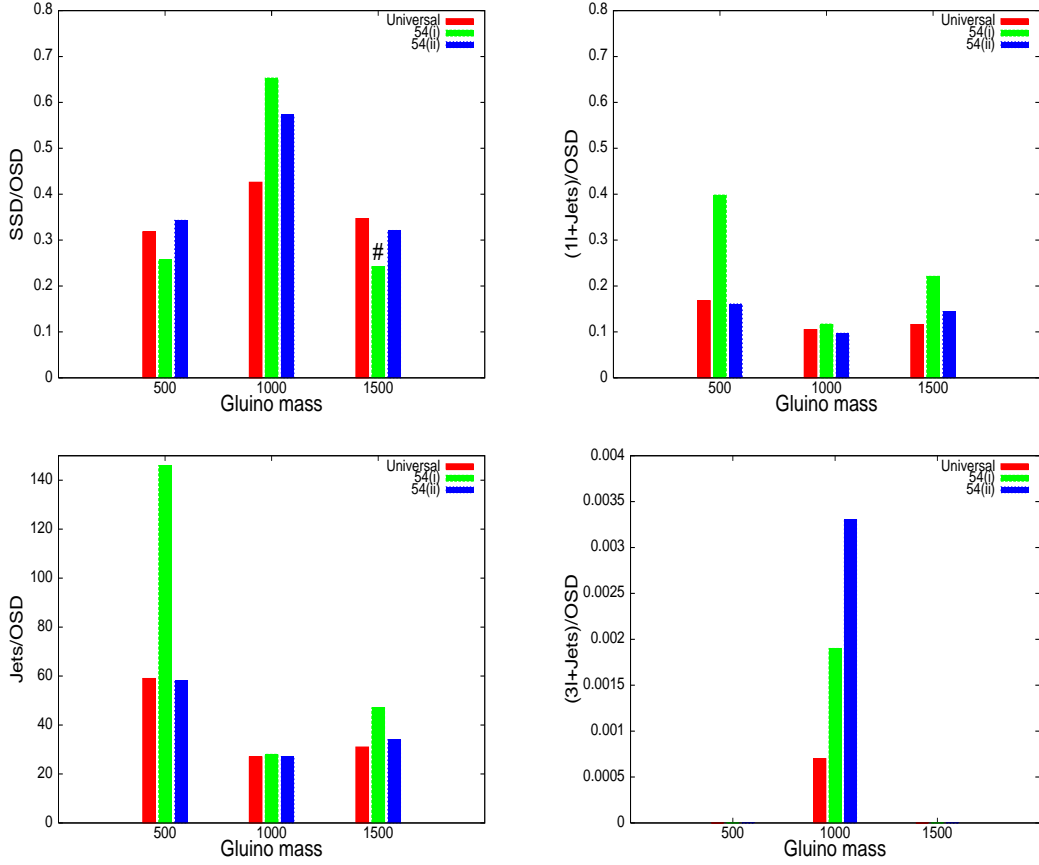


Figure 12: Event ratios for **pMSSM** in $SO(10)$: $m_{\tilde{f}} = 1000$ GeV, $\mu = 300$ GeV, $\tan \beta = 5$

4.2 Non-universal $SO(10)$ in **pMSSM** :

In this subsection we analyse some cases of gaugino non-universality arising in $SO(10)$ scenarios. As has been mentioned earlier, the gaugino mass ratios at high scale in this case depend not only on the chain of $SO(10)$ breaking but also on the presence of an intermediate breaking scale. Considering all of these will thus lead to a plethora of possibilities. Here we take an illustrative case of $SO(10)$ breaking through the lowest non-singlet representation, namely **54**, and consider two breaking chains: (i) via $SU(2) \times SO(7)$ (denoted by **54(i)**) and (ii) via $SU(4) \times SU(2)_L \times SU(2)_R$ (denoted by **54(ii)**). We also assume that there is no intermediate scale involved in the GUT breaking process [21] (See in section 2).

Our style of analysis remains the same as in the case of $SU(5)$. In figures 10 - 17 we present the predictions in the **pMSSM** framework, with the same sequence in choosing the low-energy parameters as in figures 1 - 8. Figure 18 contains our predictions for SUGRA in

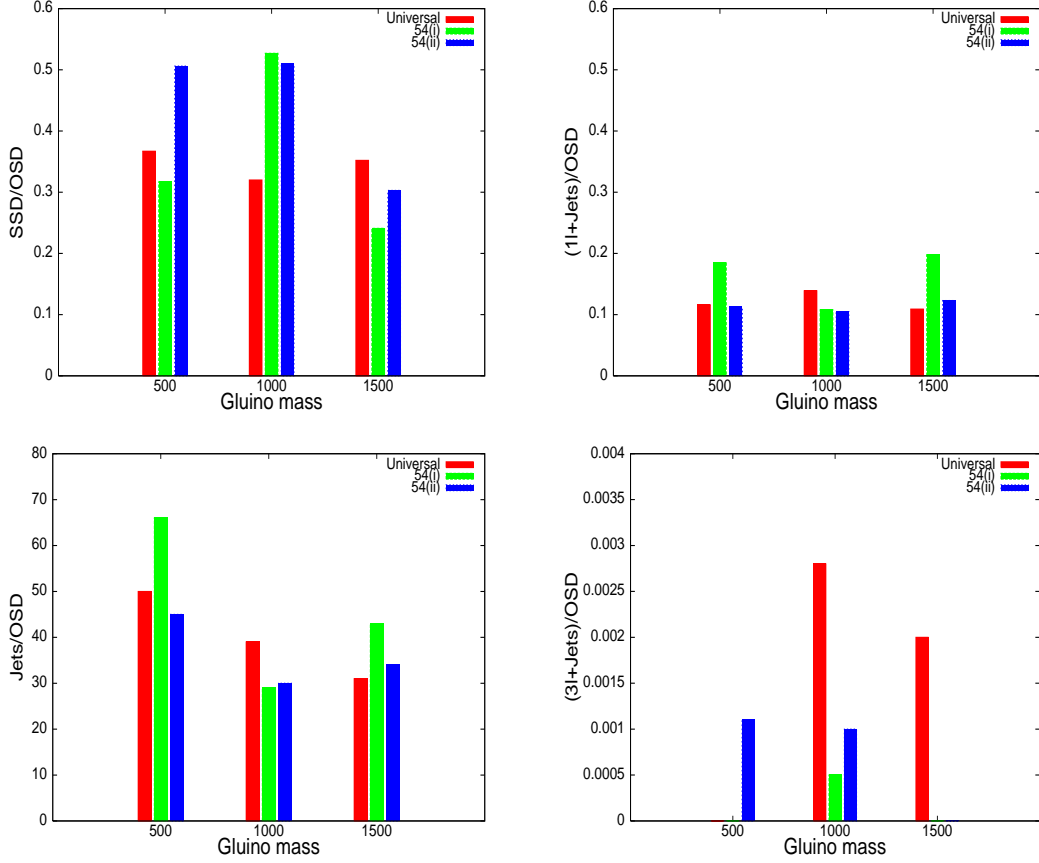


Figure 13: Event ratios for **pMSSM** in $SO(10)$: $m_{\tilde{f}}=1000$ GeV, $\mu=300$ GeV, $\tan\beta=40$

$SO(10)$, the parameters being chosen in the same fashion as in figure 9.

The observations on the different cases take very similar lines as those in the case of $SU(5)$. However, the following general features are noticed from figures 10 - 17:

1. The case of **54(i)** is largely distinguishable from the other cases through one channel or the other. This possibility is more pronounced for sfermion masses at 1000 GeV.
2. The universal case, on the other hand, shows very similar behaviour as in **54(ii)**. This is because the chargino/neutralino spectra do not show much variation between these two cases, as a result of which the absolute cross-sections, too, do not provide much of a handle. The most effective discrimination is possible through the ratio $(3\ell+jets)/OSD$ channel.
3. The dependence on $\tan\beta$ is less than in the case of $SU(5)$. This is because, as can

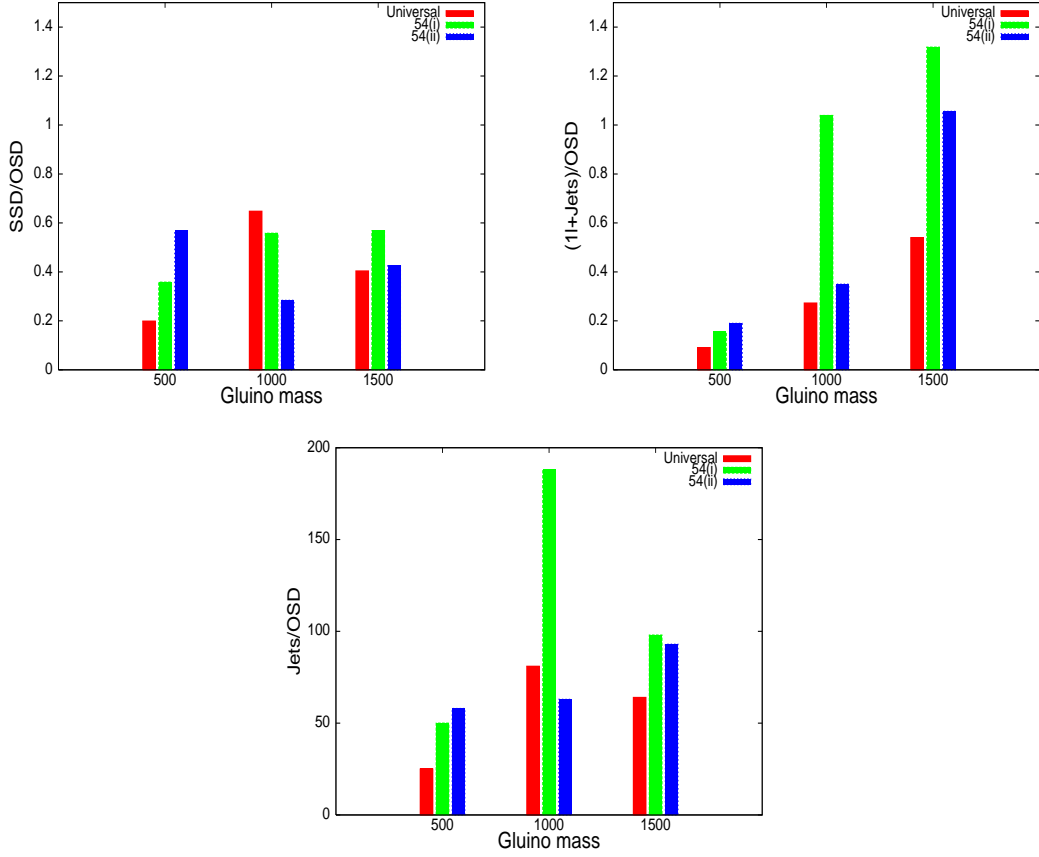


Figure 14: Event ratios for **pMSSM** in **SO(10)**: $m_{\tilde{f}} = 500$ GeV, $\mu = 1000$ GeV, $\tan \beta = 5$

be seen from Appendix A, the charginos and higher neutralinos are heavier here than in the corresponding cases with **SU(5)**. As a result, the sbottom decaying into them (which initiates cascades leading to leptons in the final state) are relatively suppressed, thus denying one the enhancement that could be seen through enhanced sbottom production rates for $\tan \beta = 40$.

4. The problem with backgrounds for single-lepton and SSD signals with heavy gluinos and sfermions, already pointed out in the case of **SU(5)** persists for **54(i)**.
5. The suppression of single lepton events is still observed, especially for low μ .
6. The results corresponding to the universal case for each point in figures 10-17 are identical with those for **SU(5)** **pMSSM** with the same parameter values. Similarly, the results for universal **SUGRA** in figure 18 are identical with those in figure 9.

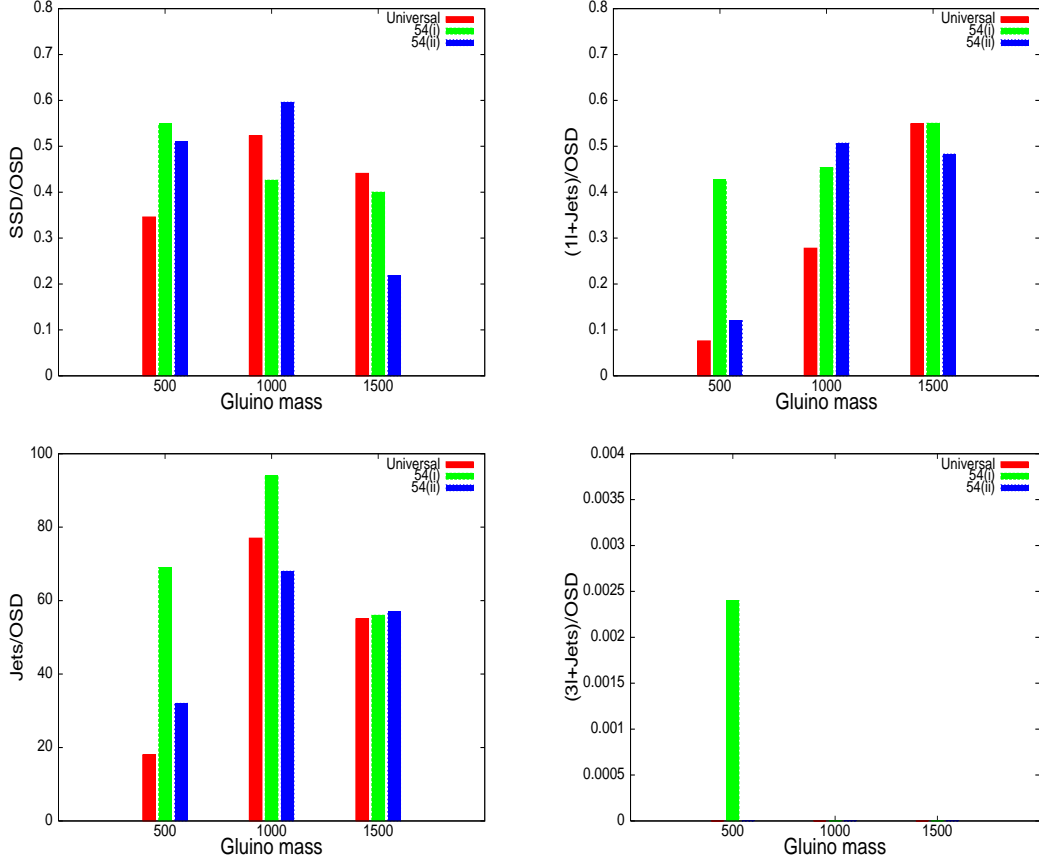


Figure 15: Event ratios for **pMSSM** in **SO(10)**: $m_{\tilde{g}}=500$ GeV, $\mu=1000$ GeV, $\tan\beta=40$

Figure 18 contains the predictions for **SO(10)** in a non-universal SUGRA setting. For $m_{\tilde{g}}=500$ GeV, the universal case may be separated from others through $(1\ell + jets)/OSD$ or $jets/OSD$ as well as through null observation of $(3\ell + jets)/OSD$, while **54(i)** may be distinguished from SSD/OSD or through $jets/OSD$. Thus, as opposed to the **pMSSM** case, all the three schemes of GUT breaking studied here are separable from each other. For $m_{\tilde{g}}=1000$ GeV, any observation of $(3\ell + jets)/OSD$ points uniquely to **54(ii)**, while the separation of the universal case and **54(i)** is difficult. For $m_{\tilde{g}}=1500$ GeV, the observables are in general drowned by backgrounds, excepting the case of **54(ii)** with $jets/OSD$ and $(3\ell + jets)/OSD$.

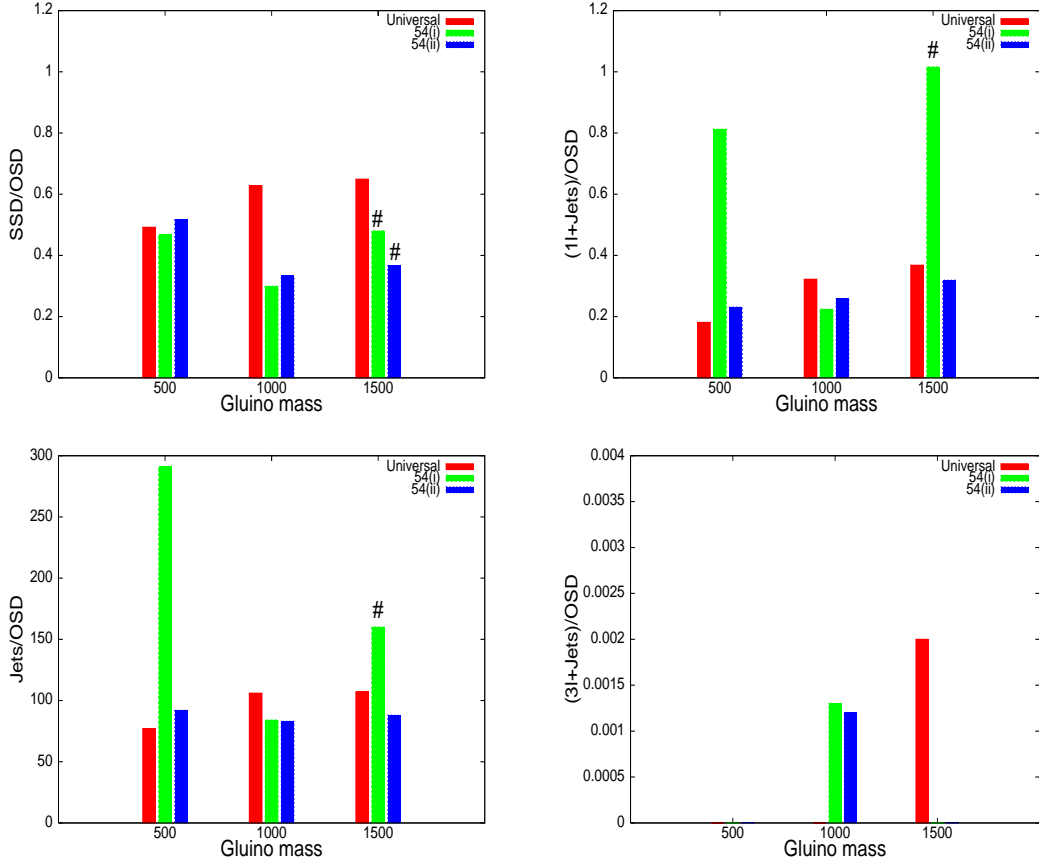


Figure 16: Event ratios for **pMSSM** in **SO(10)**: $m_{\tilde{f}} = 1000$ GeV, $\mu = 1000$ GeV, $\tan \beta = 5$

5 Summary and conclusions

We have carried out a multichannel analysis of SUSY signals, including $jets + \cancel{E}_T$, SSD, OSD, $trileptons + jets + \cancel{E}_T$ and $single\ lepton + jets + \cancel{E}_T$, for a number of non-universal representations breaking the SU(5) and SO(10) GUT groups, and compared them with those corresponding to universal gaugino masses. While all representations of SU(5) have been considered, we have confined ourselves to two breaking chains of SO(10) through **54**. Both a phenomenological SUSY spectrum for the remaining particles and one arising from a SUGRA scenario have been studied in this context.

We have found it most useful to discriminate among the various cases with the help of ratios of event rates for the various signals mentioned above, although the absolute event rates have also been presented, and can be used for specific cases. In any case the absolute

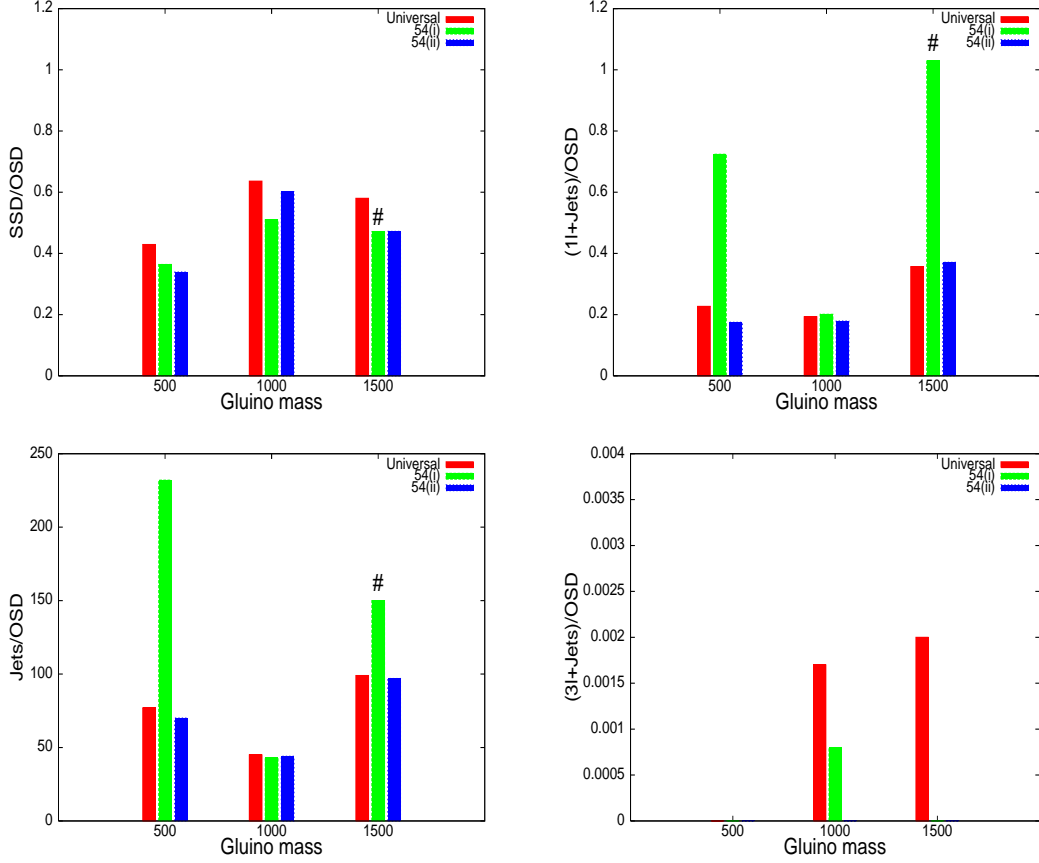


Figure 17: Event ratios for pMSSM in SO(10): $m_{\tilde{g}} = 1000$ GeV, $\mu = 1000$ GeV, $\tan \beta = 40$

event rates provide additional information which can be gainfully used in one's analysis. In general, it is found that the GUT-breaking representations are rather clearly differentiable over a substantial region of the parameter space in the case of **75** and **200** of SU(5) and **54 (i)** of SO(10). For these kinds of gaugino non-universality, distinction between an SU(5) and an SO(10) SUSY is also rather easy. For the **24** of SU(5), **54(ii)** of SO(10) and the universal case, such distinction is relatively difficult in many cases from the event ratios, and one may have to use the absolute event rates for them. However, even in these cases the ratio $(3\ell + jets)/OSD$ can be useful in discrimination, especially in separating the universal case. In general, distinction is relatively easy for high values of μ , since a low μ enhances the Higgsino component of low-lying charginos and neutralinos, thus tending to partially obliterate the clear stamps of various gaugino mass patterns as manifested in the physical states. It is also interesting to note that for the non-minimal SUGRA scenario, at $m_{\tilde{g}} = 1500$

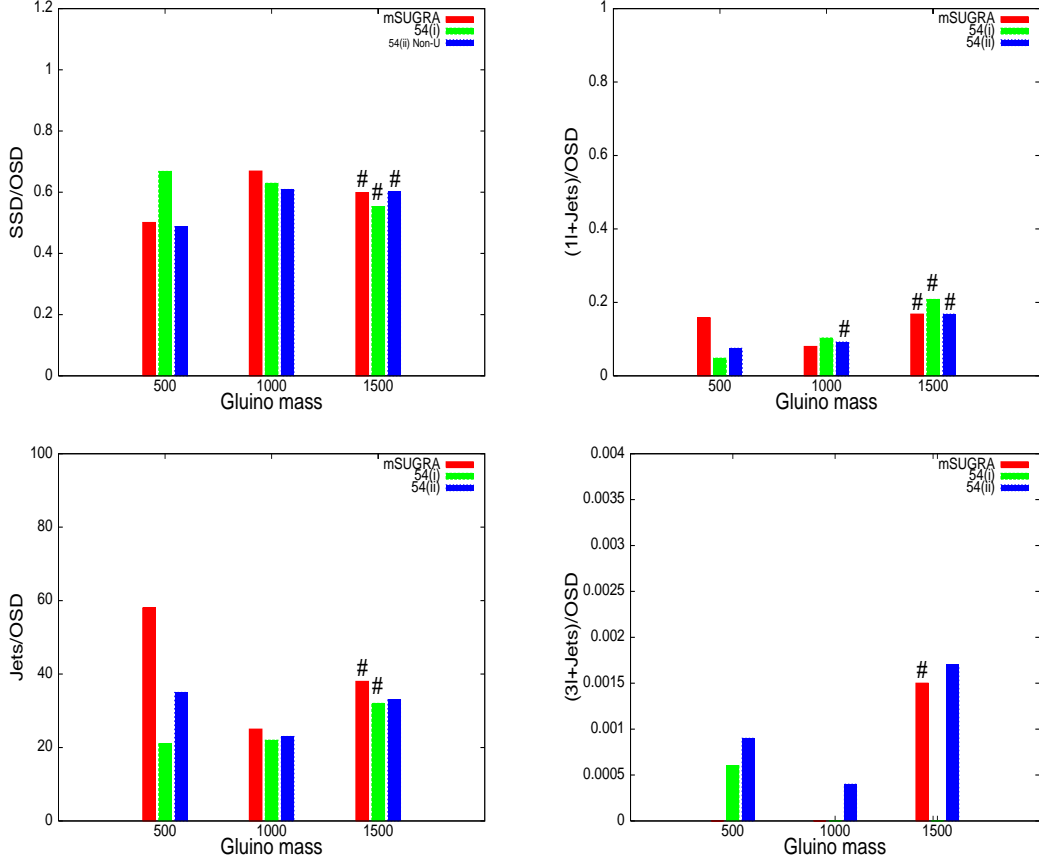


Figure 18: Event ratios for SO(10) **SUGRA** with non-universal gaugino masses: $m_0 = 506$ GeV, $\tan\beta = 5$, $sgn(\mu) = +$, $A_0 = 0$

GeV, only **24** in SU(5) and both the breaking chains of **54** in SO(10) give excess signal over background in almost all channels, while others including mSUGRA are always overwhelmed by background in OSD channel.

In the effort to learn about gaugino non-universality, one is also required to have an idea of the gluino and sfermion masses, and it is expected that various kinematic distributions (ranging from p_T to effective mass) will throw light on them in such a study. The role of such distributions (especially of missing p_T and lepton p_T) is also important when judgment has to be made on the basis of the mass separation between the two lightest neutralinos, which is a possible discriminator between **24** of SU(5) and the universal case. While the value of $\tan\beta$, another quantity affecting the observables, can be obtained from studies of the SUSY Higgs sector and Yukawa couplings, extraction of the value of the μ is a more challenging task.

One is likely to face this challenge in ascertaining the nature of gaugino non-universality, if any, unless the magnitude μ is determined by radiative electroweak symmetry breaking, as is expected in a SUGRA scenario.

It should also be noted that, in an illustrative study like this, we have used leading order cross-sections only. Higher order effects need to be taken into account in order to complete the study, although the use of ratios suggested by us can cancel the K -factors. However, our preliminary investigation serves to show that, once data from the LHC are available, a detailed look at them can indeed indicate whether some SUSY signals are consistent with specific scenarios embedded in a GUT setting. Our study is thus commensurate with the ‘inverse problem’ approach to LHC data.

On the whole, the exploration of gaugino non-universality is an extremely important task in understanding the underlying nature of a SUSY scenario. Therefore, further elaborate studies in this direction need to be undertaken in a signal-based manner.

Acknowledgment: This work was supported by funds made available by the Department of Atomic Energy, Government of India, under a Five-Year Plan Project. Computational work for this study were partially carried out at the cluster computing facility at the Harish-Chandra Research Institute (<http://cluster.mri.ernet.in>). We would like to thank Sudhir Kumar Gupta for his help in finalising our code. SB thanks Priyotosh Bandyopadhyay, Shamik Banerjee and Utpal Chattopadhyay for many useful discussions. The authors also like to acknowledge the hospitality of the Theoretical Physics Department, Indian Association for the Cultivation of Science, Kolkata, where a part the project was carried out.

References

- [1] For reviews see for example, H. E. Haber and G. L. Kane, Phys. Rept. **117**, 75 (1985); G. Kane (ed), Perspectives On Supersymmetry, *World Scientific* (1998).
- [2] S. Dawson, E. Eichten and C. Quigg, Phys. Rev. D **31**, 1581 (1985) ; X. Tata, arXiv:hep-ph/9706307.
- [3] A. V. Gladyshev and D. I. Kazakov, arXiv: hep-ph/0606288.
- [4] S. P. Martin, arXiv: hep-ph/9709356.
- [5] J. L. Bourjaily, G. L. Kane, P. Kumar and T. T. Wang, arXiv:hep-ph/0504170.

- [6] A. A. Affolder *et al.* [CDF Collaboration], Phys. Rev. Lett. **88**, 041801 (2002) [arXiv:hep-ex/0106001].
- [7] A. Datta, G. L. Kane and M. Toharia, arXiv:hep-ph/0510204.
- [8] V. D. Barger, W. Y. Keung and R. J. N. Phillips, Phys. Rev. Lett. **55**, 166 (1985) ; H. Baer, X. Tata and J. Woodside, Phys. Rev. D **41**, 906 (1990).
- [9] A. Datta, K. Kong and K. T. Matchev, Phys. Rev. D **72**, 096006 (2005) [Erratum-ibid. D **72**, 119901 (2005)] [arXiv:hep-ph/0509246].
- [10] H. Baer, X. Tata and J. Woodside, Phys. Rev. D **45**, 142 (1992) ; R. M. Barnett, J. F. Gunion and H. E. Haber, Phys. Lett. B **315**, 349 (1993) [arXiv:hep-ph/9306204].
- [11] G. Duckeck *et al.* [ATLAS Collaboration].
- [12] A. Datta and B. Mukhopadhyaya, Phys. Rev. Lett. **85**, 248 (2000) [arXiv:hep-ph/0003174] ; R. Barbier *et al.*, Phys. Rept. **420**, 1 (2005) [arXiv:hep-ph/0406039].
- [13] See for example J. L. Feng and T. Moroi, Phys. Rev. D **58**, 035001 (1998) [arXiv:hep-ph/9712499] ; J. L. Feng and T. Moroi, Phys. Rev. D **61**, 095004 (2000) [arXiv:hep-ph/9907319] ; K. Hamaguchi, M. M. Nojiri and A. de Roeck, JHEP **0703**, 046 (2007) [arXiv:hep-ph/0612060] ; S. K. Gupta, B. Mukhopadhyaya and S. K. Rai, Phys. Rev. D **75**, 075007 (2007) [arXiv:hep-ph/0701063].
- [14] N. Arkani-Hamed and S. Dimopoulos, JHEP **0506**, 073 (2005) [arXiv:hep-th/0405159].
- [15] G. F. Giudice and A. Romanino, Nucl. Phys. B **699**, 65 (2004) [Erratum-ibid. B **706**, 65 (2005)] [arXiv:hep-ph/0406088] ; N. Arkani-Hamed, S. Dimopoulos, G. F. Giudice and A. Romanino, Nucl. Phys. B **709**, 3 (2005) [arXiv:hep-ph/0409232] ; S. K. Gupta, B. Mukhopadhyaya and S. K. Rai, Phys. Rev. D **73**, 075006 (2006) [arXiv:hep-ph/0510306].
- [16] N. Bernal, A. Djouadi and P. Slavich, JHEP **0707**, 016 (2007) [arXiv:0705.1496 [hep-ph]].
- [17] S. Ambrosanio, G. L. Kane, G. D. Kribs, S. P. Martin and S. Mrenna, Phys. Rev. D **54**, 5395 (1996) [arXiv:hep-ph/9605398] ; S. Dimopoulos, S. D. Thomas and J. D. Wells, Nucl. Phys. B **488**, 39 (1997) [arXiv:hep-ph/9609434] ; G. F. Giudice and R. Rattazzi, Phys. Rept. **322**, 419 (1999) [arXiv:hep-ph/9801271].

- [18] L. Randall and R. Sundrum, Nucl. Phys. B **557**, 79 (1999) [arXiv:hep-th/9810155].
- [19] J. R. Ellis, C. Kounnas and D. V. Nanopoulos, Nucl. Phys. B **247**, 373 (1984) ;
J. R. Ellis, K. Enqvist, D. V. Nanopoulos and K. Tamvakis, Phys. Lett. B **155**, 381 (1985).
- [20] M. Drees, Phys. Lett. B **158**, 409 (1985).
- [21] N. Chamoun, C. S. Huang, C. Liu and X. H. Wu, Nucl. Phys. B **624**, 81 (2002) [arXiv:hep-ph/0110332].
- [22] A. Corsetti and P. Nath, Phys. Rev. D **64**, 125010 (2001) [arXiv:hep-ph/0003186].
- [23] E. Cremmer, B. Julia, J. Scherk, P. van Nieuwenhuizen, S. Ferrara and L. Girardello, Phys. Lett. B **79**, 231 (1978) ; E. Cremmer, B. Julia, J. Scherk, S. Ferrara, L. Girardello and P. van Nieuwenhuizen, Nucl. Phys. B **147**, 105 (1979).
- [24] D. Suematsu, arXiv:0706.3241 [hep-ph].
- [25] H. Abe, T. Kobayashi and Y. Omura, Phys. Rev. D **76**, 015002 (2007) [arXiv:hep-ph/0703044].
- [26] S. Profumo and C. E. Yaguna, Nucl. Phys. B **681**, 247 (2004) [arXiv:hep-ph/0307225].
- [27] S. Komine and M. Yamaguchi, Phys. Rev. D **63**, 035005 (2001) [arXiv:hep-ph/0007327].
- [28] S. Khalil, Phys. Lett. B **484**, 98 (2000) [arXiv:hep-ph/9910408].
- [29] G. Anderson, H. Baer, C. h. Chen and X. Tata, Phys. Rev. D **61**, 095005 (2000) [arXiv:hep-ph/9903370].
- [30] K. Huitu, Y. Kawamura, T. Kobayashi and K. Puolamaki, Phys. Rev. D **61**, 035001 (2000) [arXiv:hep-ph/9903528].
- [31] K. Huitu, J. Laamanen, P. N. Pandita and S. Roy, Phys. Rev. D **72**, 055013 (2005) [arXiv:hep-ph/0502100].
- [32] K. Choi and H. P. Nilles, JHEP **0704**, 006 (2007) [arXiv:hep-ph/0702146].
- [33] S. I. Bityukov and N. V. Krasnikov, Phys. Atom. Nucl. **65**, 1341 (2002) [Yad. Fiz. **65**, 1374 (2002)] [arXiv:hep-ph/0102179].

- [34] S. I. Bityukov and N. V. Krasnikov, arXiv:hep-ph/0210269 ; S. I. Bityukov and N. V. Krasnikov, Nuovo Cim. A **112**, 913 (1999) [arXiv:hep-ph/9903519] ; S. I. Bityukov and N. V. Krasnikov, Phys. Lett. B **469**, 149 (1999) [Phys. Atom. Nucl. **64**, 1315 (2001 YAFIA,64,1391-1398.2001)] [arXiv:hep-ph/9907257].
- [35] A. Datta, A. Datta, M. Drees and D. P. Roy, Phys. Rev. D **61**, 055003 (2000) [arXiv:hep-ph/9907444].
- [36] H. Baer, C. h. Chen, F. Paige and X. Tata, Phys. Rev. D **53**, 6241 (1996) [arXiv:hep-ph/9512383].
- [37] N. Arkani-Hamed, G. L. Kane, J. Thaler and L. T. Wang, JHEP **0608**, 070 (2006) [arXiv:hep-ph/0512190].
- [38] F. Gabbiani, E. Gabrielli, A. Masiero and L. Silvestrini, Nucl. Phys. B **477**, 321 (1996) [arXiv:hep-ph/9604387].
- [39] W. M. Yao *et al.* [Particle Data Group], J. Phys. G **33**, 1 (2006).
- [40] A. Djouadi, J. L. Kneur and G. Moultaka, Comput. Phys. Commun. **176**, 426 (2007) [arXiv:hep-ph/0211331].
- [41] S. F. King, J. P. Roberts and D. P. Roy, arXiv:0705.4219 [hep-ph].
- [42] D. G. Cerdeno and C. Munoz, JHEP **0410**, 015 (2004) [arXiv:hep-ph/0405057] ; G. Belanger, F. Boudjema, A. Cottrant, A. Pukhov and A. Semenov, Nucl. Phys. B **706**, 411 (2005) [arXiv:hep-ph/0407218].
- [43] A. Birkedal-Hansen and B. D. Nelson, Phys. Rev. D **67**, 095006 (2003) [arXiv:hep-ph/0211071] ; U. Chattopadhyay and D. P. Roy, Phys. Rev. D **68**, 033010 (2003) [arXiv:hep-ph/0304108].
- [44] F. E. Paige, S. D. Protopopescu, H. Baer and X. Tata, arXiv:hep-ph/0312045.
- [45] S. P. Martin and P. Ramond, Phys. Rev. D **48**, 5365 (1993) [arXiv:hep-ph/9306314].
- [46] A. Djouadi, M. Drees and J. L. Kneur, JHEP **0603**, 033 (2006) [arXiv:hep-ph/0602001].
- [47] T. Sjostrand, S. Mrenna and P. Skands, JHEP **0605**, 026 (2006) [arXiv:hep-ph/0603175].

- [48] P. Skands *et al.*, JHEP **0407**, 036 (2004) [arXiv:hep-ph/0311123].
- [49] H. L. Lai *et al.* [CTEQ Collaboration], Eur. Phys. J. C **12**, 375 (2000) [arXiv:hep-ph/9903282].
- [50] S. Chakrabarti, A. Datta and N. K. Mondal, Pramana **63**, 1355 (2004).
- [51] A. Pukhov, arXiv:hep-ph/0412191.
- [52] H. Baer, C. h. Chen, M. Drees, F. Paige and X. Tata, Phys. Rev. D **59**, 055014 (1999) [arXiv:hep-ph/9809223].

APPENDIX A

Here we list the neutralino and chargino masses in the region of the parameter space covered by us for all the representations. Tables A1-A8 represent mass spectra in **pMSSM** framework in SU(5) and SO(10), while table A9 is for the **SUGRA** framework. In tables A1-A8, we depict the spectra for three gluino masses namely $m_{\tilde{g}}= 500$ GeV, 1000 GeV and 1500 GeV and fixed μ , $m_{\tilde{f}}$ and $\tan\beta$. The entries marked NA do not give consistent spectra having a neutralino LSP or are disallowed by LEP limits.

Table A1 : Neutralino and Chargino spectra (GeV) for SU(5) and SO(10) **pMSSM**

$$m_{\tilde{f}} = 500 \text{ GeV}, \mu = 300 \text{ GeV}, \tan\beta = 5$$

(Figures 1 and 10)

$m_{\tilde{g}}$	Model	$m_{\tilde{\chi}_1^0}$	$m_{\tilde{\chi}_2^0}$	$m_{\tilde{\chi}_3^0}$	$m_{\tilde{\chi}_4^0}$	$m_{\tilde{\chi}_\pm 1}$	$m_{\tilde{\chi}_\pm 2}$
500	universal	66.8	128.3	305.9	330.2	126.8	329.5
500	24	37.6	209.8	312.2	323	210.8	328.3
500	75	276	294	371.1	474.1	276.4	474.2
500	200	232.73	303.83	365.66	729.01	235.36	369.37
500	54(i)	68.13	276.34	312.36	378.34	280.24	379.78
500	54(ii)	72.79	210.45	311.88	323.44	211.43	328.44
1000	universal	140.4	243.1	304.5	373.6	238.2	372.3
1000	24	75.5	291.2	309.3	474.8	294.4	475.0
1000	75	294.1	300.3	751.7	927.7	294.4	927.7
1000	200	285.47	302.46	631.27	1509.18	288.47	631.47
1000	54(i)	142.82	296.65	312.53	723.07	299.76	723.11
1000	54(ii)	148.42	292.45	308.76	475.10	294.41	475.30
1500	universal	211.42	293.78	303.64	491.75	278.76	491.42
1500	24	114.81	298.36	307.56	718.07	299.73	718.10
1500	75	296.86	300.48	1155.07	1413.08	297.09	1413.08
1500	200	292.48	301.79	951.77	2322.19	294.64	951.81
1500	54(i)	216.22	298.63	318.30	1098.88	300.77	1098.89
1500	54(ii)	224.27	302.87	306.93	710.06	299.67	710.08

Table A2: Neutralino and Chargino spectra (GeV) for SU(5) and SO(10) **pMSSM**

$$m_{\tilde{f}} = 1000 \text{ GeV}, \mu = 300 \text{ GeV}, \tan \beta = 5$$

(Figures 3 and 12)

$m_{\tilde{g}}$	Model	$m_{\tilde{\chi}^0_1}$	$m_{\tilde{\chi}^0_2}$	$m_{\tilde{\chi}^0_3}$	$m_{\tilde{\chi}^0_4}$	$m_{\tilde{\chi}^\pm_1}$	$m_{\tilde{\chi}^\pm_2}$
500	universal	68.8	131.6	305.7	330.4	130.0	329.6
500	24	38.6	213.9	312.0	323.5	215.0	328.6
500	75	277.4	295.1	379.2	481.8	277.8	482.0
500	200	235.87	303.71	368.42	746.27	238.55	371.84
500	54(i)	69.95	278.83	312.21	385.02	282.81	386.24
500	54(ii)	74.84	213.99	311.70	323.81	215.00	328.63
1000	universal	142.3	245.1	304.4	374.9	240.1	373.5
1000	24	76.5	291.7	309.2	479.3	294.8	479.5
1000	75	294.2	300.3	760.1	935.9	294.5	935.9
1000	200	285.83	302.39	636.12	1524.92	288.76	636.30
1000	54(i)	144.38	296.80	312.51	729.18	299.86	729.22
1000	54(ii)	150.16	292.92	308.64	478.87	294.81	479.05
1500	universal	212.88	294.61	303.56	494.02	279.26	493.70
1500	24	115.53	298.38	307.51	713.30	299.75	713.33
1500	75	296.92	300.46	1161.27	1419.11	297.13	1419.11
1500	200	292.6	301.75	955.63	233.44	294.72	955.67
1500	54(i)	217.29	298.68	318.41	1103.54	300.79	1103.55
1500	54(ii)	225.64	303.05	306.85	713.38	299.75	713.40

Table A3: Neutralino and Chargino spectra (GeV) for SU(5) and SO(10) **pMSSM**

$$m_{\tilde{f}} = 500 \text{ GeV}, \mu = 1000 \text{ GeV}, \tan \beta = 5$$

(Figures 5 and 14)

$m_{\tilde{g}}$	Model	$m_{\tilde{\chi}^0_1}$	$m_{\tilde{\chi}^0_2}$	$m_{\tilde{\chi}^0_3}$	$m_{\tilde{\chi}^0_4}$	$m_{\tilde{\chi}^\pm_1}$	$m_{\tilde{\chi}^\pm_2}$
500	universal	73.0	148.0	1002.2	1006.6	147.9	1006.9
500	24	37.7	228.6	1003.1	1004.9	228.6	1006.1
500	75	371.0	449.0	1002.0	1009.1	449.0	1009.5
500	200	299.19	738.18	1001.81	1011.24	299.21	1007.88
500	54(i)	73.25	354.58	1003.53	1004.71	354.59	1006.29
500	54(ii)	74.62	228.62	1003.12	1004.85	228.62	1006.15
1000	universal	149.6	302.7	1002.0	1007.9	302.7	1007.9
1000	24	NA	NA	NA	NA	NA	NA
1000	75	NA	NA	NA	NA	NA	NA
1000	200	NA	NA	NA	NA	NA	NA
1000	54(i)	150.47	716.90	1004.14	1007.33	716.94	1009.40
1000	54(ii)	151.57	462.04	1004.19	1004.27	462.05	1006.65
1500	universal	228.81	461.31	1001.78	1009.98	461.26	1009.63
1500	24	116.03	700.85	1003.8	1007.11	700.89	1009.06
1500	75	NA	NA	NA	NA	NA	NA
1500	200	NA	NA	NA	NA	NA	NA
1500	54(i)	230.56	983.92	1003.83	1117.94	985.38	1118.16
1500	54(ii)	231.35	700.91	1003.69	1007.21	700.95	1009.06

Table A4 : Neutralino and Chargino spectra (GeV) for SU(5) and SO(10) **pMSSM**

$$m_{\tilde{f}} = 1000 \text{ GeV}, \mu = 1000 \text{ GeV}, \tan \beta = 5$$

(Figures 7 and 16)

$m_{\tilde{g}}$	Model	$m_{\tilde{\chi}_1^0}$	$m_{\tilde{\chi}_2^0}$	$m_{\tilde{\chi}_3^0}$	$m_{\tilde{\chi}_4^0}$	$m_{\tilde{\chi}_1^\pm}$	$m_{\tilde{\chi}_2^\pm}$
500	universal	74.1	149.8	1002.2	1006.6	149.8	1006.8
500	24	38.2	231.4	1003.0	1004.8	465.5	1006.5
500	75	376.4	454.4	1002.2	1009.1	454.4	1009.4
500	200	302.60	748.21	1001.77	1011.38	302.62	1007.80
500	54(i)	74.33	358.80	1003.48	1004.67	358.81	1006.20
500	54(ii)	75.76	231.46	1003.26	1004.80	231.46	1006.55
1000	universal	150.9	305.0	1001.9	1007.9	305.0	1007.8
1000	24	76.8	465.5	1004.1	1004.2	465.5	1006.5
1000	75	763.2	894.0	1003.3	1042.3	894.0	1042.5
1000	200	614.03	1001.39	1009.07	1536.64	614.09	1012.64
1000	54(i)	151.60	721.34	1004.10	1007.29	721.39	1009.33
1000	54(ii)	152.91	465.37	1004.15	1004.21	465.38	1006.55
1500	universal	230.06	463.39	1001.75	1009.92	463.34	1009.54
1500	24	116.59	703.66	1003.76	1007.03	703.69	1008.95
1500	75	NA	NA	NA	NA	NA	NA
1500	200	904.54	1001.14	1045.98	2344.38	905.13	1047.34
1500	54(i)	231.64	984.71	1003.80	1121.25	986.17	1121.45
1500	54(ii)	233.01	704.02	1003.65	1007.13	704.06	1008.96

Table A5 : Neutralino and Chargino spectra (GeV) for SU(5) and SO(10) **pMSSM**

$$m_{\tilde{f}} = 500 \text{ GeV}, \mu = 300 \text{ GeV}, \tan \beta = 40$$

(Figures 2 and 11)

$m_{\tilde{g}}$	Model	$m_{\tilde{\chi}^0_1}$	$m_{\tilde{\chi}^0_2}$	$m_{\tilde{\chi}^0_3}$	$m_{\tilde{\chi}^0_4}$	$m_{\tilde{\chi}^\pm_1}$	$m_{\tilde{\chi}^\pm_2}$
500	universal	69.3	134.5	309.2	323.7	134.2	326.2
500	24	35.3	198.8	309.3	332.2	199.2	334.8
500	75	281.3	291.2	373.6	468.1	283.5	468.5
500	200	241.96	306.0	356.96	722.48	245.05	361.29
500	54(i)	69.89	266.23	309.42	386.17	268.02	387.19
500	54(ii)	70.27	198.94	309.06	332.50	199.13	334.79
1000	universal	143.3	250.3	307.0	364.7	248.6	364.8
1000	24	73.1	286.6	307.1	478.5	286.9	478.7
1000	75	295.5	300.5	750.8	925.5	297.1	925.5
1000	200	288.96	303.85	626.87	1501.91	292.89	627.07
1000	54(i)	144.95	294.75	309.58	722.85	296.05	722.89
1000	54(ii)	145.09	288.49	306.64	478.55	286.93	478.66
1500	universal	216.13	294.81	305.68	486.87	285.51	486.81
1500	24	112.51	297.31	305.75	710.55	295.87	710.58
1500	75	297.63	300.75	1153.72	1411.23	298.74	1411.23
1500	200	294.32	302.81	948.35	2314.19	297.22	948.39
1500	54(i)	219.55	297.85	314.36	1097.87	298.58	1097.88
1500	54(ii)	219.94	304.27	305.244	710.57	295.87	710.58

Table A6 : Neutralino and Chargino spectra (GeV) for SU(5) and SO(10) pMSSM

$$m_{\tilde{f}} = 1000 \text{ GeV}, \mu = 300 \text{ GeV}, \tan \beta = 40$$

(Figures 4 and 13)

$m_{\tilde{g}}$	Model	$m_{\tilde{\chi}^0_1}$	$m_{\tilde{\chi}^0_2}$	$m_{\tilde{\chi}^0_3}$	$m_{\tilde{\chi}^0_4}$	$m_{\tilde{\chi}^\pm_1}$	$m_{\tilde{\chi}^\pm_2}$
500	universal	71.3	137.8	309.0	323.9	137.5	326.2
500	24	36.3	202.9	309.1	332.9	203.3	335.4
500	75	282.5	292.5	381.7	476.3	284.7	476.6
500	200	254.4	305.84	360.0	741.6	248.60	364.0
500	54(i)	71.72	268.66	309.30	390.94	270.45	391.84
500	54(ii)	72.23	203.11	308.88	333.26	203.30	335.39
1000	universal	144.7	251.8	306.9	365.4	250.0	365.4
1000	24	73.9	287.2	307.0	482.1	287.5	482.3
1000	75	295.7	300.7	758.3	932.9	297.2	932.9
1000	200	289.26	302.18	1279.9	3148.39	298.5	1279.9
1000	54(i)	146.47	294.93	309.54	728.67	296.19	728.71
1000	54(ii)	146.76	289.12	306.53	482.16	287.46	482.26
1500	universal	217.50	295.43	305.6	488.9	285.91	488.83
1500	24	112.73	297.44	305.67	713.34	295.97	713.37
1500	75	297.54	301.07	1416.72	1577.18	298.76	1416.72
1500	200	294.43	302.77	952.30	2326.64	297.28	952.34
1500	54(i)	220.66	297.91	314.41	1102.44	298.62	1102.45
1500	54(ii)	220.49	304.43	305.17	713.75	295.98	713.76

Table A7 : Neutralino and Chargino spectra (GeV) for SU(5) and SO(10) **pMSSM**

$$m_{\tilde{f}} = 500 \text{ GeV}, \mu = 1000 \text{ GeV}, \tan \beta = 40$$

(Figures 6 and 15)

$m_{\tilde{g}}$	Model	$m_{\tilde{\chi}_1^0}$	$m_{\tilde{\chi}_2^0}$	$m_{\tilde{\chi}_3^0}$	$m_{\tilde{\chi}_4^0}$	$m_{\tilde{\chi}_1^\pm}$	$m_{\tilde{\chi}_2^\pm}$
500	universal	73.0	149.0	1003.5	1005.0	149.0	1006.5
500	24	NA	NA	NA	NA	NA	NA
500	75	NA	NA	NA	NA	NA	NA
500	200	299.23	732.41	1002.83	1008.35	299.25	1007.09
500	54(i)	73.26	349.6	1003.53	1005.47	349.61	1007.11
500	54(ii)	73.30	224.59	1003.64	1004.85	224.59	1006.62
1000	universal	149.4	303.7	1003.1	1005.9	303.7	1007.1
1000	24	NA	NA	NA	NA	NA	NA
1000	75	NA	NA	NA	NA	NA	NA
1000	200	NA	NA	NA	NA	NA	NA
1000	54(i)	150.40	709.85	1003.10	1011.17	709.88	1012.32
1000	54(ii)	150.09	457.27	1003.14	1006.60	457.27	1007.85
1500	universal	228.57	462.53	1002.78	1007.48	462.52	1008.27
1500	24	NA	NA	NA	NA	NA	NA
1500	75	NA	NA	NA	NA	NA	NA
1500	200	NA	NA	NA	NA	NA	NA
1500	54(i)	NA	NA	NA	NA	NA	NA
1500	54(ii)	NA	NA	NA	NA	NA	NA

Table A8 : Neutralino and Chargino spectra (GeV) for SU(5) and SO(10) **pMSSM**

$$m_{\tilde{f}} = 1000 \text{ GeV}, \mu = 1000 \text{ GeV}, \tan \beta = 40$$

(Figures 8 and 17)

$m_{\tilde{g}}$	Model	$m_{\tilde{\chi}^0_1}$	$m_{\tilde{\chi}^0_2}$	$m_{\tilde{\chi}^0_3}$	$m_{\tilde{\chi}^0_4}$	$m_{\tilde{\chi}^\pm_1}$	$m_{\tilde{\chi}^\pm_2}$
500	universal	74.2	151.1	1003.4	1005.9	151.1	1006.5
500	24	37.3	227.4	1003.6	1004.8	227.4	1006.6
500	75	327.7	454.2	1003.5	1006.8	454.2	1008.1
500	200	303.39	744.63	1002.79	1008.48	303.4	1007.02
500	54(i)	74.39	354.00	1003.5	1005.45	354.01	1007.07
500	54(ii)	74.52	227.66	1003.60	1004.82	227.67	1006.56
1000	universal	150.8	306.1	1003.0	1005.9	306.1	1007.0
1000	24	75.7	460.1	1003.2	1006.5	460.6	1007.8
1000	75	758.4	899.7	1005.2	1033.5	900.0	1034.3
1000	200	615.17	1002.19	1006.76	1528.79	615.21	1010.41
1000	54(i)	151.65	714.62	1003.08	1011.24	714.65	1012.37
1000	54(ii)	151.43	460.59	1003.11	1006.58	460.60	1007.80
1500	universal	229.98	464.89	1002.76	1007.45	464.89	1008.22
1500	24	115.55	697.57	1002.82	1010.87	697.59	1011.80
1500	75	NA	NA	NA	NA	NA	NA
1500	200	NA	NA	NA	NA	NA	NA
1500	54(i)	231.57	976.77	1002.85	1126.06	977.49	1126.21
1500	54(ii)	230.95	697.53	1002.74	1011.01	697.54	1011.80

Table A9 : Neutralino and Chargino spectra (GeV) for SU(5) and SO(10) **SUGRA**

$$m_{\tilde{f}} = 506 \text{ GeV at } M_{GUT}, \tan \beta = 5$$

(Figures 9 and 18)

$m_{\tilde{g}}$	Model	$m_{\tilde{\chi}_1^0}$	$m_{\tilde{\chi}_2^0}$	$m_{\tilde{\chi}_3^0}$	$m_{\tilde{\chi}_4^0}$	$m_{\tilde{\chi}_1^\pm}$	$m_{\tilde{\chi}_2^\pm}$
500	universal	70.74	129.16	289.03	316.94	127.91	314.65
500	24	42.54	199.39	252.60	288.42	200.04	289.92
500	75	136.36	147.69	400.26	470.33	138.90	467.43
500	200	202.80	249.30	348.56	792.82	207.99	348.32
500	54(i)	66.97	169.16	196.78	376.84	169.85	372.59
500	54(ii)	80.32	199.26	251.2	288.21	199.52	289.38
1000	universal	171.20	321.40	555.60	574.93	321.55	573.38
1000	24	92.52	420.53	445.10	545.27	413.17	538.06
1000	75	NA	NA	NA	NA	NA	NA
1000	200	414.84	433.79	686.93	1767.96	421.96	680.06
1000	54(i)	158.55	251.39	271.43	795.42	245.44	785.1
1000	54(ii)	179.6	419.19	442.6	544.84	411.23	537.62
1500	universal	275.57	519.73	819.60	834.40	520.22	833.47
1500	24	145.87	624.14	638.06	831.61	608.20	818.44
1500	75	NA	NA	NA	NA	NA	NA
1500	200	592.68	603.33	1059.96	2804.17	602.40	1048.06
1500	54(i)	244.91	291.76	321.48	1234.77	281.58	1220.69
1500	54(ii)	285.17	620.81	633.83	831.08	604.33	817.89

APPENDIX B

In this appendix we tabulate the cross-sections in each channel for all representations of SU(5) and SO(10) in the region of parameter space studied and depicted in figures 1-18. The cross-sections are named as follows: σ_1 for OSD, σ_2 for SSD, σ_3 for $(1\ell + jets)$, σ_4 for $jets$ and σ_5 for $(3\ell + jets)$. The points for which we do not get consistent spectra are denoted by NA as earlier and the points which give null result (for $(3\ell + jets)$ channel only) is written as NULL. Bold faced entries correspond to cross-sections which are less than 2σ above the background for an integrated luminosity of 300 fb^{-1} .

Table B1 : Cross-sections (pb) for SU(5) and SO(10) **pMSSM**

$$m_{\tilde{f}} = 500 \text{ GeV}, \mu = 300 \text{ GeV}, \tan\beta = 5$$

(Figures 1 and 10)

$m_{\tilde{g}}$	Model	σ_1	σ_2	σ_3	σ_4	σ_5
500	universal	0.3434	0.1157	0.0472	18.3140	NULL
500	24	0.4648	0.1223	0.0552	20.2893	NULL
500	75	0.0388	0.0185	0.0178	2.0555	NULL
500	200	0.0576	0.0240	0.0133	5.5483	NULL
500	54(i)	0.3682	0.0970	0.0440	16.8908	NULL
500	54(ii)	0.4456	0.1291	0.0483	18.3423	NULL
1000	universal	0.1086	0.0261	0.0152	3.4062	NULL
1000	24	0.0808	0.0340	0.0133	4.0154	NULL
1000	75	0.0089	0.0063	0.0054	1.3613	NULL
1000	200	0.0090	0.0072	0.0048	1.4017	NULL
1000	54(i)	0.0446	0.0180	0.0114	2.8733	NULL
1000	54(ii)	0.0745	0.0316	0.0103	3.2941	NULL
1500	universal	0.0346	0.0845	0.0512	0.7688	NULL
1500	24	0.0265	0.0096	0.0040	1.2308	NULL
1500	75	0.0037	0.0010	0.0020	0.2852	NULL
1500	200	0.0034	0.0019	0.0026	0.3110	NULL
1500	54(i)	0.0167	0.0060	0.0033	0.6066	NULL
1500	54(ii)	0.0239	0.0057	0.0036	0.6256	NULL

Table B2 : Cross-sections (pb) for SU(5) and SO(10) pMSSM

$$m_{\tilde{f}} = 1000 \text{ GeV}, \mu = 300 \text{ GeV}, \tan \beta = 5$$

(Figures 3 and 12)

$m_{\tilde{g}}$	Model	σ_1	σ_2	σ_3	σ_4	σ_5
500	universal	0.1400	0.0440	0.0230	8.3310	NULL
500	24	0.1317	0.0463	0.0207	8.7260	NULL
500	75	0.0108	0.0048	0.0064	3.3280	NULL
500	200	0.0137	0.0068	0.0079	4.5549	NULL
500	54(i)	0.0600	0.0154	0.0239	8.7907	NULL
500	54(ii)	0.1396	0.0479	0.0225	8.1194	NULL
1000	universal	0.0310	0.0132	0.0033	0.8462	2.0×10^{-5}
1000	24	0.0350	0.0196	0.0034	0.9417	5.0×10^{-5}
1000	75	0.0197	0.0137	0.0040	0.8528	NULL
1000	200	0.0145	0.0091	0.0027	0.7410	3.0×10^{-5}
1000	54(i)	0.0371	0.0242	0.0044	1.0666	7.0×10^{-5}
1000	54(ii)	0.0397	0.0228	0.0038	1.0930	0.0001
1500	universal	0.0091	0.0032	0.0010	0.2788	NULL
1500	24	0.0089	0.0037	0.0015	0.3422	NULL
1500	75	0.0006	0.0003	0.0006	0.1023	NULL
1500	200	0.0016	0.0006	0.0007	0.1259	NULL
1500	54(i)	0.0037	0.0009	0.0008	0.1766	NULL
1500	54(ii)	0.0090	0.0029	0.0013	0.3120	NULL

Table B3 : Cross-sections (pb) for SU(5) and SO(10) pMSSM

$$m_{\tilde{f}} = 500 \text{ GeV}, \mu = 1000 \text{ GeV}, \tan \beta = 5$$

(Figures 5 and 14)

$m_{\tilde{g}}$	Model	σ_1	σ_2	σ_3	σ_4	σ_5
500	universal	0.7456	0.1483	0.0680	18.8841	NULL
500	24	0.3510	0.1814	0.0537	19.1663	NULL
500	75	0.0356	0.0013	0.0013	0.1100	NULL
500	200	0.0125	0.0075	0.0106	0.9345	NULL
500	54(i)	0.2831	0.1015	0.0439	14.3062	NULL
500	54(ii)	0.2979	0.1694	0.0567	17.4439	0.0007
1000	universal	0.0453	0.0293	0.0124	3.6705	NULL
1000	24	NA	NA	NA	NA	NA
1000	75	NA	NA	NA	NA	NA
1000	200	NA	NA	NA	NA	NA
1000	54(i)	0.0102	0.0057	0.0107	1.9349	NULL
1000	54(ii)	0.0337	0.0096	0.0118	2.1440	0.0001
1500	universal	0.0090	0.0036	0.0049	0.5811	NULL
1500	24	0.0062	0.0031	0.0066	0.4968	NULL
1500	75	NA	NA	NA	NA	NA
1500	200	NA	NA	NA	NA	NA
1500	54(i)	0.0036	0.0020	0.0047	0.3528	NULL
1500	54(ii)	0.0045	0.0019	0.0048	0.4229	NULL

Table B4 : Cross-sections (pb) for SU(5) and SO(10) pMSSM

$$m_{\tilde{f}} = 1000 \text{ GeV}, \mu = 1000 \text{ GeV}, \tan \beta = 5$$

(Figures 7 and 16)

$m_{\tilde{g}}$	Model	σ_1	σ_2	σ_3	σ_4	σ_5
500	universal	0.1022	0.0503	0.0185	7.9664	NULL
500	24	0.0878	0.0449	0.0255	8.7054	NULL
500	75	0.0047	0.0009	0.0017	0.7335	NULL
500	200	0.0028	0.0019	0.0038	2.5958	NULL
500	54(i)	0.0302	0.0141	0.0245	8.8041	NULL
500	54(ii)	0.0879	0.0454	0.0203	8.1171	NULL
1000	universal	0.0098	0.0062	0.0032	1.0422	NULL
1000	24	0.0119	0.0037	0.0032	1.0220	NULL
1000	75	0.0044	0.0005	0.0004	0.1052	NULL
1000	200	0.0002	0.0001	0.0006	0.2546	NULL
1000	54(i)	0.0119	0.0035	0.0027	0.9998	1.0×10^{-5}
1000	54(ii)	0.0125	0.0043	0.0032	1.0401	1.5×10^{-5}
1500	universal	0.0026	0.0017	0.0009	0.2781	0.5×10^{-5}
1500	24	0.0036	0.0012	0.0010	0.3007	NULL
1500	75	NA	NA	NA	NA	NA
1500	200	6.0×10^{-5}	6.0×10^{-5}	0.0001	0.0172	NULL
1500	54(i)	0.0006	0.0003	0.0006	0.1023	NULL
1500	54(ii)	0.0034	0.0012	0.0011	0.2959	NULL

Table B5 : Cross-sections (pb) for SU(5) and SO(10) pMSSM

$$m_{\tilde{f}} = 500 \text{ GeV}, \mu = 300 \text{ GeV}, \tan\beta = 40$$

(Figures 2 and 11)

$m_{\tilde{g}}$	Model	σ_1	σ_2	σ_3	σ_4	σ_5
500	universal	0.5220	0.2281	0.0729	16.0476	0.0008
500	24	0.6831	0.3310	0.0581	18.3674	NULL
500	75	0.0393	0.0203	0.0215	1.0915	NULL
500	200	0.0983	0.0393	0.0222	2.4881	NULL
500	54(i)	0.5987	0.2071	0.0632	14.6693	NULL
500	54(ii)	0.5995	0.2563	0.0617	15.1236	NULL
1000	universal	0.1033	0.0244	0.0142	3.3959	0.0003
1000	24	0.0800	0.0300	0.0156	4.2959	NULL
1000	75	0.0089	0.0041	0.0060	1.3822	NULL
1000	200	0.0083	0.0032	0.0048	1.3759	NULL
1000	54(i)	0.0569	0.0161	0.0146	3.0397	NULL
1000	54(ii)	0.0653	0.0254	0.0131	3.5114	NULL
1500	universal	0.0374	0.0071	0.0058	0.7133	NULL
1500	24	0.0306	0.0101	0.0056	1.4278	0.0001
1500	75	0.0027	0.0009	0.0030	0.2765	NULL
1500	200	0.0023	0.0012	0.0027	0.3046	NULL
1500	54(i)	0.0273	0.0048	0.0056	0.5729	NULL
1500	54(ii)	0.0266	0.0055	0.0054	0.6889	NULL

Table B6 : Cross-sections (pb) for SU(5) and SO(10) pMSSM

$$m_{\tilde{f}} = 1000 \text{ GeV}, \mu = 300 \text{ GeV}, \tan \beta = 40$$

(Figures 4 and 13)

$m_{\tilde{g}}$	Model	σ_1	σ_2	σ_3	σ_4	σ_5
500	universal	0.1602	0.0059	0.0019	8.1530	NULL
500	24	0.1714	0.0745	0.0236	8.4541	NULL
500	75	0.0312	0.0234	0.0085	2.8467	NULL
500	200	0.0258	0.0139	0.0097	3.9270	NULL
500	54(i)	0.1264	0.0400	0.0233	8.3948	NULL
500	54(ii)	0.1706	0.0864	0.0193	7.7990	0.0002
1000	universal	0.0214	0.0069	0.0030	0.8446	6.0×10^{-5}
1000	24	0.0343	0.0175	0.0037	1.0486	0.0001
1000	75	0.0182	0.0106	0.0043	0.8455	3.0×10^{-5}
1000	200	0.0120	0.0063	0.0027	0.7075	NULL
1000	54(i)	0.0368	0.0194	0.0040	1.0739	2.0×10^{-5}
1000	54(ii)	0.0359	0.0183	0.0038	1.0810	4.0×10^{-5}
1500	universal	0.0088	0.0031	0.0009	0.2799	2.0×10^{-5}
1500	24	0.0082	0.0038	0.0013	0.3403	NULL
1500	75	0.0004	0.0003	0.0006	0.0981	NULL
1500	200	0.0015	0.0006	0.0008	0.1272	NULL
1500	54(i)	0.0039	0.0009	0.0008	0.1700	NULL
1500	54(ii)	0.0090	0.0027	0.0011	0.3157	NULL

Table B7 : Cross-sections (pb) for SU(5) and SO(10) pMSSM
 $m_{\tilde{f}} = 500 \text{ GeV}$, $\mu = 1000 \text{ GeV}$, $\tan\beta = 40$
(Figures 6 and 15)

$m_{\tilde{g}}$	Model	σ_1	σ_2	σ_3	σ_4	σ_5
500	universal	0.9410	0.3260	0.0715	17.3778	NULL
500	24	NA	NA	NA	NA	NA
500	75	NA	NA	NA	NA	NA
500	200	0.0283	0.0225	0.0193	1.6686	NULL
500	54(i)	0.2766	0.1517	0.1182	19.2174	0.0007
500	54(ii)	0.6048	0.3087	0.0725	19.3995	NULL
1000	universal	0.0467	0.0245	0.0130	3.6043	NULL
1000	24	NA	NA	NA	NA	NA
1000	75	NA	NA	NA	NA	NA
1000	200	NA	NA	NA	NA	NA
1000	54(i)	0.0217	0.0092	0.0098	2.0479	NULL
1000	54(ii)	0.0308	0.0183	0.0156	2.1147	NULL
1500	universal	0.0100	0.0044	0.0055	5.5373	NULL
1500	24	NA	NA	NA	NA	NA
1500	75	NA	NA	NA	NA	NA
1500	200	NA	NA	NA	NA	NA
1500	54(i)	NA	NA	NA	NA	NA
1500	54(ii)	NA	NA	NA	NA	NA

Table B8 : Cross-sections (pb) for SU(5) and SO(10) pMSSM

$$m_{\tilde{f}} = 1000 \text{ GeV}, \mu = 1000 \text{ GeV}, \tan \beta = 40$$

(Figures 8 and 17)

$m_{\tilde{g}}$	Model	σ_1	σ_2	σ_3	σ_4	σ_5
500	universal	0.1027	0.0440	0.0233	7.9509	NULL
500	24	0.1123	0.0373	0.0243	8.7752	0.0002
500	75	0.0059	0.0019	0.0010	0.8054	NULL
500	200	0.0023	0.0018	0.0053	2.5620	NULL
500	54(i)	0.0379	0.0138	0.0274	8.7898	NULL
500	54(ii)	0.1161	0.0394	0.0203	8.1907	NULL
1000	universal	0.0204	0.0130	0.0039	0.9343	3.0×10^{-5}
1000	24	0.0209	0.0124	0.0043	0.9690	1.5×10^{-5}
1000	75	0.0314	0.0001	0.0004	0.0771	NULL
1000	200	0.0018	0.0016	0.0010	0.1095	NULL
1000	54(i)	0.0182	0.0929	0.0037	0.7876	1.5×10^{-5}
1000	54(ii)	0.0216	0.0130	0.0038	0.9677	NULL
1500	universal	0.0028	0.0016	0.0010	0.2775	0.6×10^{-5}
1500	24	0.0030	0.0014	0.0013	0.3063	NULL
1500	75	NA	NA	NA	NA	NA
1500	200	NA	NA	NA	NA	NA
1500	54(i)	0.0007	0.0003	0.0007	0.1044	NULL
1500	54(ii)	0.0024	0.0007	0.0009	0.2052	NULL

Table B9 : Cross-sections (pb) for SU(5) and SO(10) **SUGRA**

$$m_{\tilde{f}} = 506 \text{ GeV at } M_{GUT}, \tan \beta = 5$$

(Figures 9 and 18)

$m_{\tilde{g}}$	Model	σ_1	σ_2	σ_3	σ_4	σ_5
500	universal	0.2818	0.1411	0.0445	16.5239	NULL
500	24	0.3807	0.1900	0.0390	16.1696	0.0007
500	75	0.3685	0.3382	0.0282	10.1572	0.0003
500	200	0.0912	0.0667	0.0194	9.0323	NULL
500	54(i)	0.6041	0.4034	0.0293	13.1929	0.0004
500	54(ii)	0.4153	0.2023	0.0313	14.7555	0.0004
1000	universal	0.0397	0.0266	0.0032	1.0060	NULL
1000	24	0.0315	0.0191	0.0029	0.8035	0.0001
1000	75	NA	NA	NA	NA	NA
1000	200	0.0137	0.0105	0.0013	0.4504	2.0×10^{-5}
1000	54(i)	0.0312	0.0196	0.0032	0.7153	NULL
1000	54(ii)	0.0321	0.0195	0.0029	0.7662	1.0×10^{-5}
1500	universal	0.0019	0.0011	0.0003	0.0735	3.0×10^{-5}
1500	24	0.0022	0.0012	0.0004	0.0750	2.0×10^{-5}
1500	75	NA	NA	NA	NA	NA
1500	200	0.0012	0.0009	0.0002	0.0368	2.0×10^{-5}
1500	54(i)	0.0017	0.0009	0.0004	0.0561	NULL
1500	54(ii)	0.0215	0.0013	0.0004	0.0728	4.0×10^{-5}